Liver-targeting of liposomes modified with β-sitosterol glucoside for cancer chemotherapy

Kumi Kawano

CONTENTS

List of Publication

1. Efficiency of liposomes surface-modified with soybean-derived sterylglucoside as a liver targeting carrier in HepG2 cells: Yoshie Maitani, Kumi Kawano, Kazuyo Yamada, Tsuneji Nagai, and Kozo Takayama, *J. Control. Release*, 75, 381-389 (2001). <presented in Chapter 1 of this dissertation>.

2. Liver targeting liposomes containing β-sitosterol glucoside with regard to penetration-enhancing effect on HepG2 cells: Kumi Kawano, Kouji Nakamura, Kyoko Hayashi, Tsuneji Nagai, Kozo Takayama, and Yoshie Maitani, *Biol. Pharm. Bull.*, 25 (6), 766-770 (2002). <presented in Chapter 2 of this dissertation>.

3. Preparation and pharmacokinetics of pirarubicin loaded dehydration-rehydration vesicles: Kumi Kawano, Kozo Takayama, Tsuneji Nagai, and Yoshie Maitani, *Int. J. Pharm.*, in press, <presented in Chapter 3 this dissertation>.

Abbreviations

AF	asialofetuin
ASGP-R	asialoglycoprotein receptor
AUC	area under the concentration-time curve
BSA	bovine serum albumin
Ch	cholesterol
DiI	1,1'-dioctadecyl-3,3,3',3'-tetramethylindocarbocyanine perchlorate
DMSO	dimethyl sulfoxide
DPPC	dipalmitoylphosphatidylcholine
DRV	dehydration-rehydration vesicles
DXR	doxorubicin
EPC	purified egg yolk lecithin
FBS	fetal bovine serum
FD-4	fluorescein isothiocyanate dextran 4,400
FITC	fluorescein isothiocyanate
F-THP	free pirarubicin
Gal-BSA	FITC-labeled galactosylated bovine serum albumin
Glu-BSA	FITC-labeled glucosylated bovine serum albumin
HBSS	Hank's balanced salt solution
HPLC	high performance liquid chromatography
ILS	increase in life span
L-THP	Sit-G-liposomes entrapping pirarubicin
MLV	multilamellar vesicles
OA	oleic acid

PBS	phosphate-buffered saline solution
RES	reticuloendothelial system
REV	reverse-phase evaporation vesicles
SG	soybean-derived sterylglucoside
SG-liposomes	liposomes modified with SG
Sit-G	β-sitosterol β-D-glucoside
Sit-G-liposomes	liposomes modified with Sit-G
SUV	small unilamellar vesicles
THP	pirarubicin

GENERAL INTRODUCTION

Cancer is a serious medical and social problem. In recent years, the rate of death from cancer increased in Japan, and cancer has been the highest cause of death from 1981. Furthermore, aged society of Japan will increase the occasion of cancer. The marked medical progresses reach some kinds of cancers being cured. However, others still leave the difficulty in detection and treatment.

Primary liver cancer is usually considered a highly malignant tumor with a poor prognosis. This is a rare type of cancer in Western countries, but occurs frequently in Africa and Asia since liver cancer is often sequel to viral hepatitis and cirrhosis. Furthermore, the liver is the most common target of the hematogenous metastasis in primary gastrointestinal tumors. The prognosis for liver metastasis is also extremely poor.

The best current treatment of liver cancer is surgical removal of the primary tumor if it is at an early stage and resectable. Patients with advanced non-resectable tumor are treated with local administration of anticancer drugs, such as hepatic intra-arterial chemotherapy or transarterial chemoembolization, since the most anticancer drugs are not liver-specific and often exhibit undesirable toxicity. To reduce the adverse effects and to increase the antitumor effects of anticancer drugs, drug delivery system (DDS) using the particulate drug targeting carriers, such as micelles [1], emulsions [2], microparticles [3] and liposomes [4, 5] has been investigated to deliver the drugs selectively to cancer.

Liposomes, defined as lipid bilayer vesicles, have attracted considerable interest as a potential drug carrier [6,7]. Liposome morphology and classification are shown in Figure 1 and Table 1. Liposomes are classified by their size and the number of bilayers, such as multilamellar vesicles (MLV), large unilamellar vesicles (LUV) and small unilamellar vesicles (SUV), and by their preparation methods, such as reverse-phase evaporation vesicle method (REV) and dehydration-rehydration vesicle method (DRV). As liposomes are consisted mainly from phospholipid and cholesterol, they are safety drug carriers in point of biocompatibility, antigenicity, biodegradability and toxicity. They, consisting of lipid layers with an inside water phase, can encapsulate both water soluble and lipophilic drugs. Furthermore, modification of liposome surface using ligand, such as antibody [8], protein[9] or sugar residue [10, 11], is easy to increase the selectivity of drug carriers. However,

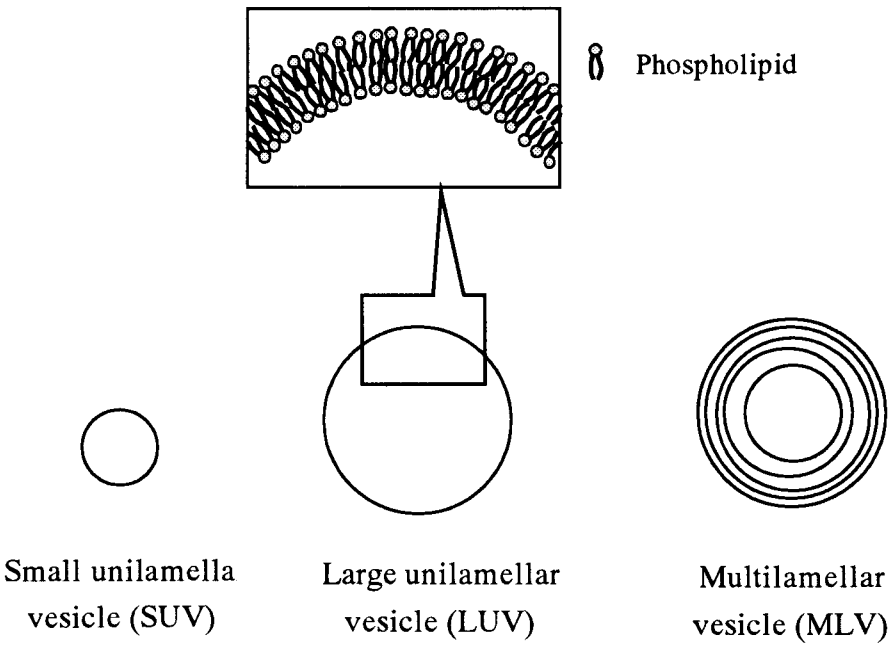

Figure 1. Morphology of different liposome structure

Table 1. Liposome classification

A. Based on structural parameters	
MLV	Multilamellar vesicles
SUV	Small unilamellar vesicles
LUV	Large unilamellar vesicles
B. Based on method of liposome preparation	
REV	Reverse-phase evaporation vesicles
DRV	Dehydration-rehydration vesicles

large particles (>0.4 μm) are commonly cleared by the reticuloendothelial system (RES), mainly Kupffer cells in liver and splenic macrophages, after intravenous administration. Also it is difficult to obtain the high entrapment of drug in the small sized liposomes by the conventional preparation method.

To deliver drugs to specific cell types, receptor-mediated endocytosis is a promising strategy. Some cell-specific receptors, such as transferrin receptor [9], folate receptor [12], lipoprotein receptor [13] and carbohydrate receptor [11] are utilized for site-specific delivery of drugs. For targeting to the hepatocytes, galactose modification of liposomes has been used, because the asialoglycoprotein receptor (ASGP-R), which recognizes galactose residue, is known to be present only on hepatocyte [14] with a high density [15]. Galactose-terminated compounds, such as lactosylceramide [16], asialofetuin [17] or synthetic glycolipids [18] have been used to modify liposomes for selective accumulation in the liver, i.e., targeting hepatocytes.

Soybean-derived sterylglucoside (SG) is obtained by extraction of soybean oil and its chemical structure is shown in Figure 2. SG has a potential for liver targeting ligand, because compared with liposome composed of phospholipid and cholesterol, liposomes modified with SG (SG-liposomes) were accumulated in liver parenchymal cells and increased antitumor effect of doxorubicin (DXR) in mice bearing M5076 metastatic liver tumors and rats bearing primary liver cancer by the result of accumulation of DXR in the liver (Tables 2 and 3) [19]. SG-liposomes have glucose residue on the surface of liposomes [20], which is essential for selective accumulation in liver cells. Recognition of glucose residue in liver cells *via* ASGP-R was reported in several papers [21, 22], in which the recognition of glucose residue was different from spacers connecting sugar and macromolecule. Glucose residue of SG does not

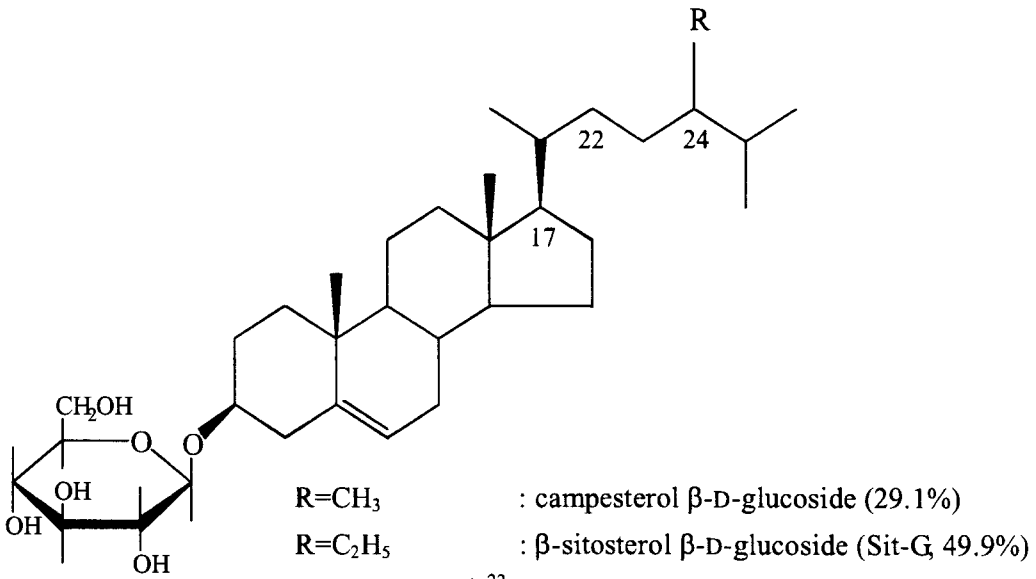

Figure 2. Chemical structures of soybean-derived sterylglucoside (SG)

The numbers in parentheses represent the ratio in SG

Table 2 Antitumor effect of SG-liposomes entrapping DXR in mice bearing M5076 liver metastasis and in rats with primary liver cancer at a dose of 5 mg/kg

Treatment	Mean (S.D.)		Median survival time (days)	% ILS [a)]
Liver metastasis of M5076				
Saline	11.4 (1.6)	**	11.5	
Free DXR	13.1 (3.1)		12.5	9.1
SG-liposomes	18.2 (10.2)		14.5	27.3
Primary liver cancer				
Saline	25.8 (17.1)	*	27.5	
Free DXR	19.7 (14.1)	**	14.0	-49.1
SG-liposomes	48.2 (23.3)		53.0	92.7

[a)] Percentage increase in life span, [(T/C-1) × 100 (%)], where T and C represent the median survival time (days) of the treated and control animals, respectively. *: $p<0.05$, **: $p<0.01$, significantly different.

K. Shimizu et al. Biol. Pharm. Bull. 21, 741-746 (1998)

have such a spacer and therefore, the underlying mechanism for selective recognition of glucose residues in SG-liposomes by liver cells is not clearly understood.

SG and β-sitosterol glucoside (Sit-G), a major component of SG, have been also reported as effective penetration enhancers of drugs across mucosal membranes by increasing the cell membrane fluidity [23]. Bile salt and glycyrrhizin are known to act as penetration enhancers in the intestinal [24], nasal [25, 26] and transdermal [27] absorption of drugs, and also as ligands for drug delivery to the liver by their specific affinities to hepatocytes [28, 29].

Thus the penetration-enhancing effect of free SG or Sit-G on

Table 3 Tissue AUC values after i.v. injection of SG-liposomes entrapping DXR in mice bearing M5076 at a dose of 5 mg/kg

Formulation	Tissue AUC [a] (μg·h/g)					
	Serum [b]	Liver (Tumor)	Heart	Lung	Kidney	Spleen (Tumor)
Free DXR	17.93 (1.05)	190.66 (23.82)	44.36 (4.20)	20.17 (3.30)	28.61 (4.57)	87.46 (26.35)
SG-liposomes	283.73 *** (19.90)	462.16 *** (67.81)	32.73 (7.02)	17.31 (3.60)	36.48 (3.40)	219.44 * (84.38)

[a] AUC values were calculated for 0-24 h (n=3-7). [b] Serum AUC is given as μg·h/mL (n=3-5). The numbers in parentheses represent S.D. *: $p<0.05$, ***$p<0.001$, significantly different from free DXR.

K. Shimizu et al. Biol. Pharm. Bull. 21, 741-746 (1998)

hepatocytes cannot be neglected, because they might be released by the degradation of SG-liposomes in the blood circulation or by Kupffer cells after intravenous injection. To elucidate the mechanism, the interaction of SG and Sit-G with hepatocyte was examined in human hepatoma cell line HepG2 as a ligand and a penetration enhancer.

To enhance the therapeutic efficacy for liver cancer using liposomes modified with Sit-G (Sit-G-liposomes), a DXR derivative, pirarubicin (4'-*O*-tetrahydropyranyldoxorubicin; THP, Figure 3) was selected because it has higher efficacy against several solid tumors, acute leukemia and malignant lymphoma [30, 31], and a lower incidence of side effects (e.g. cardiotoxicity, alopecia and gastrointestinal disorder) compared with DXR [31, 32]. The higher cellular accumulation of THP was reported since THP shows higher lipophilicity than DXR [33]. However, the conventional preparation method of liposomes was unsuitable for THP because the entrapment efficiency of drug was low, and the size of

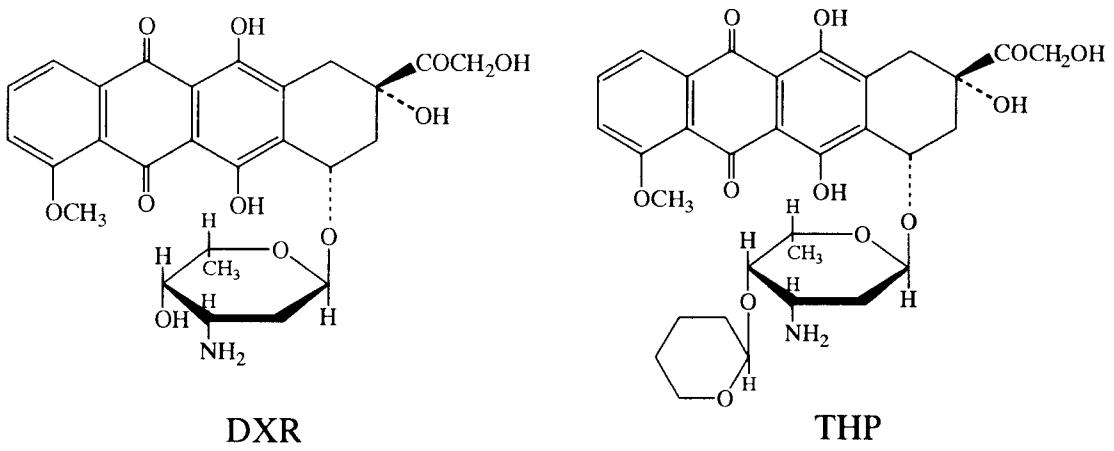

Figure 3. Chemical structures of doxorubicin (DXR) and pirarubicin (THP)

liposomes was large. The dehydration-rehydration vesicle (DRV) method[34] can entrap the drugs regardless of the molecular size and other characteristics, but the size of liposomes was the relatively large, which is not suitable for intravenous injection. To overcome this drawback, sugars are used in preparations, which improve the particle size as small as injectable size. Liposomes prepared by the DRV method can be stored in a lyophilized state, which improve shelf-life stability of liposomes used as drug carriers. Therefore, to prepare liposomes entrapping THP, DRV method was applied with some modification.

The aim of this work is to evaluate the drug targeting effect of SG-liposomes to the liver, and to increase the therapeutic efficacy for liver cancer.

In Chapter 1, the efficiency of SG-liposomes to liver targeting was evaluated in HepG2 cells, focusing mainly on the ASGP-R mediated endocytosis. In Chapter 2, the possibility that Sit-G works as a penetration enhancer in the liver was estimated by measuring the

association of FITC-dextran 4,400 (FD-4) with HepG2 cells. In Chapter 3, Sit-G-liposomes entrapping THP (L-THP) was prepared by DRV method, and their pharmacokinetics and antitumor effects were evaluated in mice bearing liver metastasis tumor.

CHAPTER 1

Efficiency of Liposomes Modified with Sterylglucoside as Liver Targeting Carrier

1. Introduction

For selective delivery of drugs to the liver parenchymal cells, galactose modification has been used, because the asialoglycoprotein receptor (ASGP-R) is known to be present only on hepatocytes [14] with a high density [15]. The schematic representation of the architecture of the liver is shown in Figure 4. Carriers modified with galactose residue, which can pass through the fenestrae in liver sinusoid, are recognized by the ASGP-R on the surface parenchymal cells and are incorporated into the cells by endocytosis. Once a ligand binds to the receptor, the ligand-receptor complex is rapidly internalized and the receptor recycles back to the surface [35], allowing high binding capacity and efficient uptake of galactosylated ligands by liver cells. These characteristics are suitable for cellular drug delivery and thus utilized for delivering interferon [36],

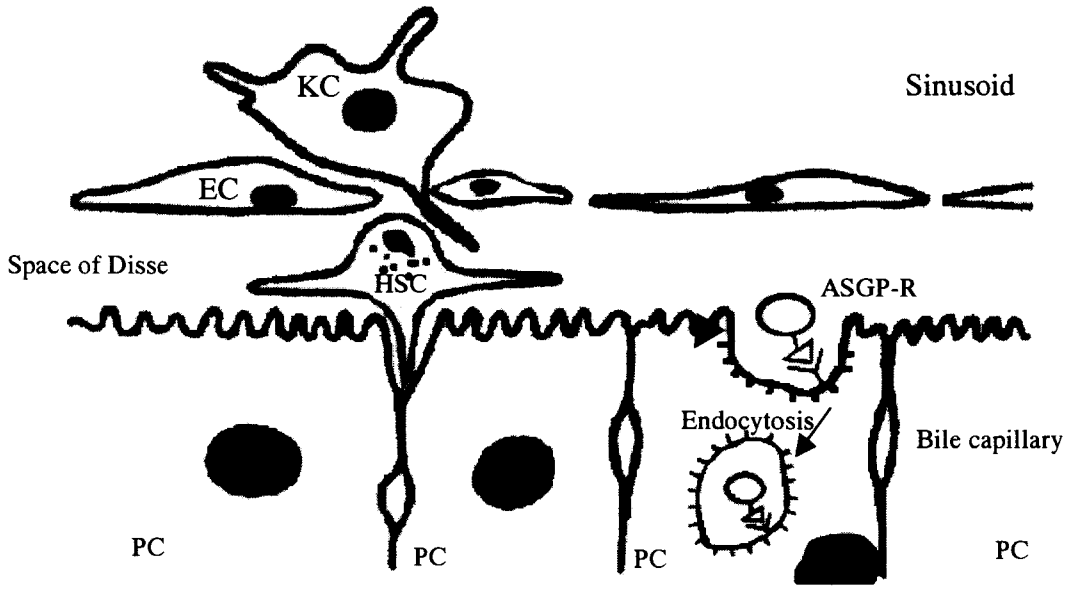

Figure 4. Schematic representation of the architecture of the liver.

EC: endothelial cells, KC: Kupffer cells, HSC: hepatic stellate cells, PC: parenchymal cells, ASGP-R: asialoglycoprotein receptor

vitamin E [17] or DNA [37, 38] to hepatocyte.

As the efficiency of a liver targeting carrier, it is important that entrapping drugs in liposomes are highly concentrated in hepatocytes. Unlike drug conjugated polymers and drug entrapped in galactose-modified liposomes having a high affinity to ASGP-R, the fate of drug entrapped in SG-liposomes might be different from carriers, i.e., SG-liposomes.

In this chapter, to evaluate the efficiency of SG-liposomes to liver targeting, the interaction of SG-liposomes with the cultured human hepatoblastoma cell line, HepG2, was investigated with emphasis on the involvement of ASGP-R mediated endocytosis. The efficiency of SG-liposomes as drug carrier was examined by measuring the association of each SG-liposomes entrapping 1,1'-dioctadecyl-3,3,3',3'-tetramethyl-indocarbocyanine perchlorate (DiI) as a marker of liposome, carboxylated polystyrene microspheres (Fluoresbrite) as a model not taken up in cells and DXR.

2. Experimental section

2.1. Materials

Dipalmitoylphosphatidylcholine (DPPC) and SG were supplied by NOF (Tokyo, Japan) and Ryukakusan Co. (Tokyo, Japan), respectively. Cholesterol (Ch), asialofetuin (AF) and daunorubicin were purchased from Sigma Chemical Co. (St. Louis, MO, USA). 1,1'-dioctadecyl-3,3,3',3'-tetramethylindocarbocyanine perchlorate (DiI) was purchased from Lambda Probes & Diagnostics (Graz, Austria). Fluoresbrite, yellow green carboxylate polystyrene microspheres of nominal size (50 nm in diameter), was purchased from Polysciences Ltd. (Warrington, PA, USA). Doxorubicin (DXR) was purchased from Wako Pure Chemicals Industries Ltd. (Osaka, Japan). RPMI 1640 medium and fetal bovine serum (FBS) were purchased from Life Technologies, Inc. (Grand Island, NY, USA). Fluorescein isothiocyanate (FITC)-labeled galactosylated bovine serum albumin (Gal-BSA) and glucosylated BSA (Glu-BSA) were purchased from EY Laboratories, Inc. (San Mateo, CA, USA). All other chemicals were of reagent grade.

2.2. Preparation of liposomes

The liposomes were prepared from DPPC, Ch (DPPC: Ch = 6:4, molar ratio, control liposomes) and SG (DPPC: Ch: SG= 6:3:1, molar ratio, SG-liposomes). Liposomes entrapping DiI or DXR were prepared by the reverse-phase evaporation vesicle (REV) method as reported previously [39]. Briefly, the lipid mixture was dissolved in chloroform and the solvent was

evaporated. In the experiment indicated, the liposome membrane was labeled by the addition of 0.4 mol% DiI to the lipid mixtures before solvent evaporation. The dried lipid film was redissolved in chloroform and isopropylether and mixed with 3 mL of 1/10 diluted phosphate-buffered saline (PBS consisting of 8.10 mM Na_2HPO_4, 1.47 mM KH_2PO_4, 137 mM NaCl and 2.68 mM KCl, pH 7.5, 1/10PBS) for DiI or 300 mM citric acid buffer (pH 4.0) for DXR. The mixture was sonicated with a bath-type sonicator (Honda Electronics, Tokyo, Japan) to give an emulsion and the organic solvents in the emulsion were evaporated to form a liposome suspension. Liposomes were extruded through a 0.2 μm polycarbonate membrane (Nuclepore, Pleasanton, CA, USA) at about 60°C. The mean diameter of SG-liposomes entrapping DiI was 227.4 nm, determined using a dynamic laser light scattering instrument (Model ELS-800, Ostuka Electronics Co., Ltd., Osaka, Japan). All of the DiI was entrapped in liposomes measuring by gel filtration.

Liposomes entrapping Fluoresbrite were prepared by the ethanol injection method [40] because polystyrene is resistant to ethanol but not to chloroform. Briefly, lipids were dissolved in ethanol and injected into preheated (about 60°C) 1/10 PBS containing Fluoresbrite. This suspension was then placed on a rotary evaporator and ethanol was evaporated to obtain the liposome suspension. Fluoresbrite entrapped in the liposomes was used without adjustment of the size of liposomes and the size of the liposomal Fluoresbrite was mean diameter 539.2 nm. The trapping efficiency of Fluoresbrite could not be calculated, because liposomal Fluoresbrite could not be separated from its free form by

ultracentrifugation.

DXR was entrapped in the liposomes by the pH gradient loading method [41]. Briefly, the pH of the liposome suspension (initially pH 4.0) was raised to pH 7.8 with 1 N NaOH solution. Then the liposome suspension was heated to 60°C and mixed with a preheated (60°C) solution of DXR in Hepes buffer (pH 7.8). The mixture was incubated with periodic mixing for 15 min at 60°C. The mean diameter of SG-liposomes entrapping DXR was 224.3 nm and approximately 98% of DXR was entrapped in SG-liposomes measuring by ultracentrifugation.

The concentration of the liposome suspension was represented by the DPPC concentrations determined by enzymatic assays (Phospholipid B Test Wako, Wako Pure Chemical Industries Ltd., Osaka, Japan).

2.3. Cell culture and cell preparation

A human hepatoblastoma cell line HepG2 (obtained from Riken Cell Bank, Ibaraki, Japan) was maintained in the RPMI 1640 medium supplemented with 10% (v/v) heat-inactivated (56°C, 30 min) FBS and 10 mM Hepes buffer in a humidified incubator (5% CO_2) at 37°C. The cells were scraped off by trypsin-EDTA (0.05% trypsin, 53 mM EDTA・4Na) and plated in 12-well tissue culture plates (3×10^5 cells) one day before the experiment. The cells were washed three times with fresh serum-free RPMI 1640 medium immediately before the experiment.

2.4. Binding and cell association assays

The binding experiments were carried out at 4°C, or cell

association at 37°C in 1 mL of serum-free RPMI 1640 medium containing the indicated concentrations of liposome. More than 99% of the cells were viable at the end of the incubation periods as determined by the Trypan blue exclusion test. Incubation was terminated by washing the plates with ice-cold PBS three times. The washed cells were lysed in PBS containing 0.2% Triton X-100.

2.5. Determination of cellular association of DiI, Fluoresbrite and DXR

The amounts of DiI, Fluoresbrite or DXR recovered from the cell fraction were determined as described below.

The fluorescence intensity of DiI was assayed using a fluorophotometer (Hitachi F-4010, Tokyo, Japan) with excitation and emission wavelengths at 550 and 570 nm, respectively. The amounts of Gal- and Glu-BSA (FITC-labeled) were measured with excitation and emission wavelengths at 490 and 520 nm, respectively. For the measurement of the fluorescence intensity of Fluoresbrite, the cell lysate was diluted in 1,2-dimethoxyethane before measuring with excitation at 458 nm and emission at 497 nm.

The amount of DXR was measured using high performance liquid chromatography (HPLC) [19]. The HPLC system consisted of a Shimadzu SCL-10A system controller, LC-10AS liquid chromatograph, SIL-10A auto injector, RF-10A$_{XL}$ fluorescence detector (excitation, 470 nm; emission, 585 nm) and YMC-Pack C18 column. The mobile phase was methanol/water/acetic acid (50/45/5, v/v/v) with a flow rate of 1.0 mL/min.

Measurements were made using the ratio of an internal standard (daunorubicin).

Protein was measured using a bicinchonic acid (BCA) protein assay kit (Pierce Chemical Co., Rockford, IL, USA). The amounts of DXR and Fluoresbrite were presented as the associated amount per mg cellular protein, and that of DiI was presented as the associated amount of liposome (DPPC) per mg cellular protein.

2.6. Statistical analysis

Data were compared using analysis of variance and Student's *t*-test. A *p*-value of 0.05 or 0.01 was considered significant.

3. Results and Discussion

3.1. Effect of AF on uptake of Gal-BSA and Glu-BSA

First, the presence of ASGP-R mediated endocytosis in HepG2 cells was confirmed using BSA modified with galactose (Gal-BSA), which is recognized as a specific ligand for ASGP-R with characteristics of high affinity for isolated liver cells [42] and a cultured hepatoblastoma cell line[43]. HepG2 is a human hepatoblastoma cell line that is known to express ASGP-R [44]. The ASGP-R on the surface of hepatocytes recognizes the galactose residue of desialylated serum protein. The galactose residue is, therefore, used for targeting drugs to liver parenchyma cells *in vivo* [45].

Figure 5 shows the amount of Gal- and Glu-BSA recovered from HepG2 cells after incubation at 4°C or 37°C with or without AF. Binding to the cell surface occurs at 4°C but internalization does not. The total amount of the association was compared with the binding amount on the cells. The amount of Gal-BSA remaining with HepG2 cells at 37°C was significantly higher than that of at 4°C ($p<0.05$). The association of Gal-BSA was increased with incubation time (from 1 to 6 h) when HepG2 cells were incubated with Gal-BSA at 37°C (data not shown). It was decreased significantly to a lower level observed at 4°C by the addition of 1 mg/mL AF, a competitor for the ASGP-R. It is well established that AF competes with galactose residue for the specific recognition by ASGP-R and thereby inhibits ASGP-R mediated endocytosis [43, 46]. These results indicated that the recognition of galactose residue by ASGP-R on HepG2 cells was inhibited by incubation with AF.

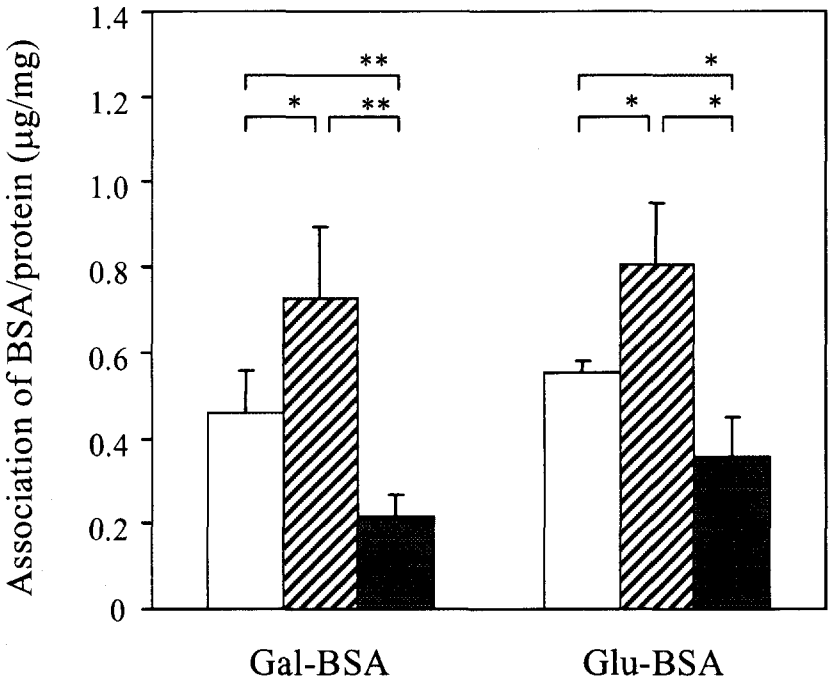

Figure 5. Association of Gal- or Glu-BSA with HepG2 cells

HepG2 cells (3×10^5 cells) were incubated with 10 μg/mL of Gal- or Glu-BSA for 2 h at 4°C (open bar) or at 37°C in the absence (hatched bar) or presence (closed bar) of 1 mg/mL AF. Each value represents the mean±S.D. (n=3-4) *:$p<0.05$, **:$p<0.01$, significantly different.

The association of BSA modified with glucose (Glu-BSA) was also measured to compare the difference of association between galactose and glucose residue. The amount of Glu-BSA recovered from HepG2 at 37°C was higher than that of Glu-BSA at 4°C and was similar to the level of Gal-BSA at 37°C. The addition of 1 mg/mL AF also affected the recovered amount of Glu-BSA significantly ($p<0.05$). These results indicated that the glucose residue have possibility to be recognized by ASGP-R. It is reported that Gal-BSA was taken up *via* ASGP-R regardless of the kind of spacer, but recognition of glucose residue was affected by the character of spacers, i.e., only glucose residue with a positively charged group in proximity to the sugar was effectively taken

up by the isolated hepatocytes [21] and hepatocytes in mice [22] *via* ASGP-R. These results were corresponded well with their findings, as Glu-BSA used in this study had similar spacer [22]. The association of Glu-BSA was compared to that of SG-liposomes in HepG2 cells because SG does not have such a spacer.

3.2. Association of DiI and Fluoresbrite entrapped in SG-liposomes with HepG2 cells

To examine the association of liposome membrane as a drug carrier, the association of the lipid layer components of liposomes with HepG2 cells using a lipophilic fluorescent marker, DiI, incorporated in SG-liposomes. Figure 6 shows that the association of DiI entrapped in SG-liposomes when they were incubated for 1 h with HepG2 cells at 4°C or 37°C in the absence or presence of AF. In the case of SG-liposomes, the amount of DiI remaining with the cells was significantly ($p<0.01$) higher when it was incubated at 37°C than at 4°C (5.7% of that added at 37°C). The SG-liposomes labeled with DiI showed sufficient association with HepG2 cells incubated for 1 h at 37°C and the amount of association was same until 6 h (data not shown). The association of DiI in SG-liposomes was increased with concentration of liposomes (from 30 to 100 μM as DPPC) incubated at 37°C for 1 h (data not shown). AF significantly ($p<0.05$) reduced the associated amount of DiI in SG-liposomes. The association of DiI was not affected by temperature or the presence of AF when it was loaded in control liposomes.

Control liposomes were not internalized because no difference between the associations of DiI in control liposomes incubated at 4°C and at 37°C (Figure 6). The DiI in SG-liposomes showed significantly higher association with HepG2 at 37°C than that of control liposomes. In Figure 5, addition of AF reduced the association of Gal- and Glu-BSA lower than that of at 4°C and it seemed that AF might inhibit the binding of both glycosyl-BSA to ASGP-R. The DiI in SG-liposomes was significantly inhibited by the presence of AF but similar level to that of at 4°C. It suggested that the interaction of SG-liposomes with ASGP-R might be weak than that of glycosyl-BSA. These findings suggest that a part of SG-liposomes were taken up by HepG2 cells *via* the ASGP-R or at least *via* the AF sensitive pathway.

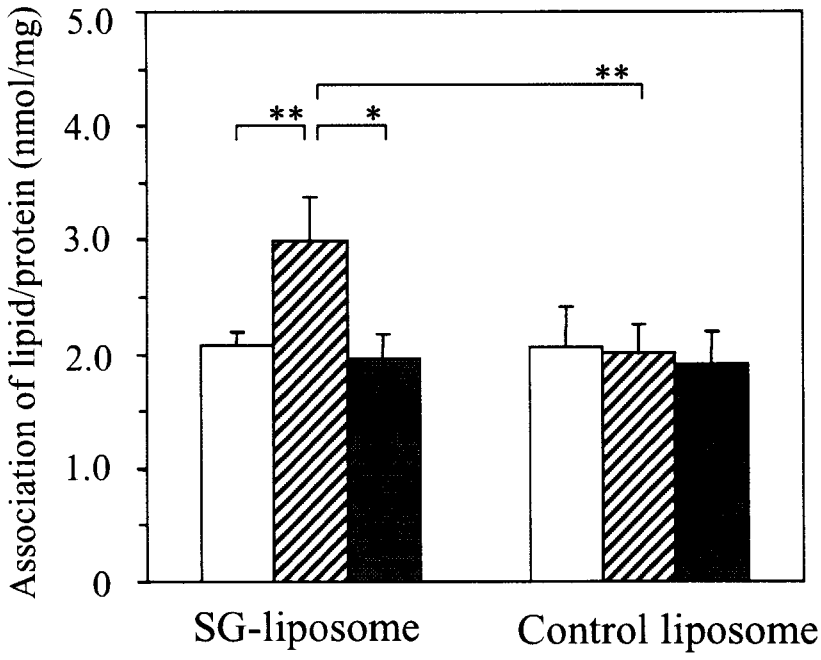

Figure 6. Association of DiI in SG- or control liposomes with HepG2 cells

HepG2 cells (3×10^5 cells) were incubated for 1 h with SG-liposomes labeled with DiI (100 μM as DPPC) at 4°C (open bar) or at 37°C in the absence (hatched bar) or presence (closed bar) of 1 mg/mL AF. Control is liposomes without SG.
Each value represents the mean±S.D. (n=3) *:$p<0.05$, **:$p<0.01$, significantly different.

As an example of compounds entrapped in liposomes, the behavior of Fluoresbrite was examined. When the cells were incubated with free Fluoresbrite for 2 h at concentrations ranging from 5 to 50 μg/mL, the amount of cell-associated Fluoresbrite was unchanged between incubation at 4°C and 37°C (data not shown), indicating this negative charged microsphere were not taken up by HepG2 cells like a negative charged plasmid DNA. The uptake of Fluoresbrite alone was negligible whereas the uptake of Fluoresbrite by the cells was increased when it was added as the SG-liposome-entrapped form (Figure 7). The association of Fluoresbrite entrapped in SG-liposomes was increased with liposome concentration (from 50 to 100 μM as DPPC) and was significantly higher than that of control liposomes (data not shown). The associated amount of Fluoresbrite was significantly higher when it was incubated at 37°C than at 4°C (39.5% of that added at 37°C for 2 h) and was increased with incubation time within observed period. AF significantly ($p<0.01$) decreased it to a similar or lower level observed at 4°C when the cells were incubated for 2 and 3 h, respectively.

The uptake of Fluoresbrite in SG-liposomes was higher at 37°C and a portion was inhibited by AF. These findings suggest that Fluoresbrite behaves like the lipid component of SG-liposomes and is incorporated in HepG2 cells *via* the AF sensitive pathway. It also suggests that SG-liposomes is an effective candidate carrier as a gene delivery system to hepatocytes. Indeed, in previous reports, the transfection by SG-liposomes entrapping plasmid DNA was significantly observed compared with control liposomes in HepG2 cells [47] and mice [48].

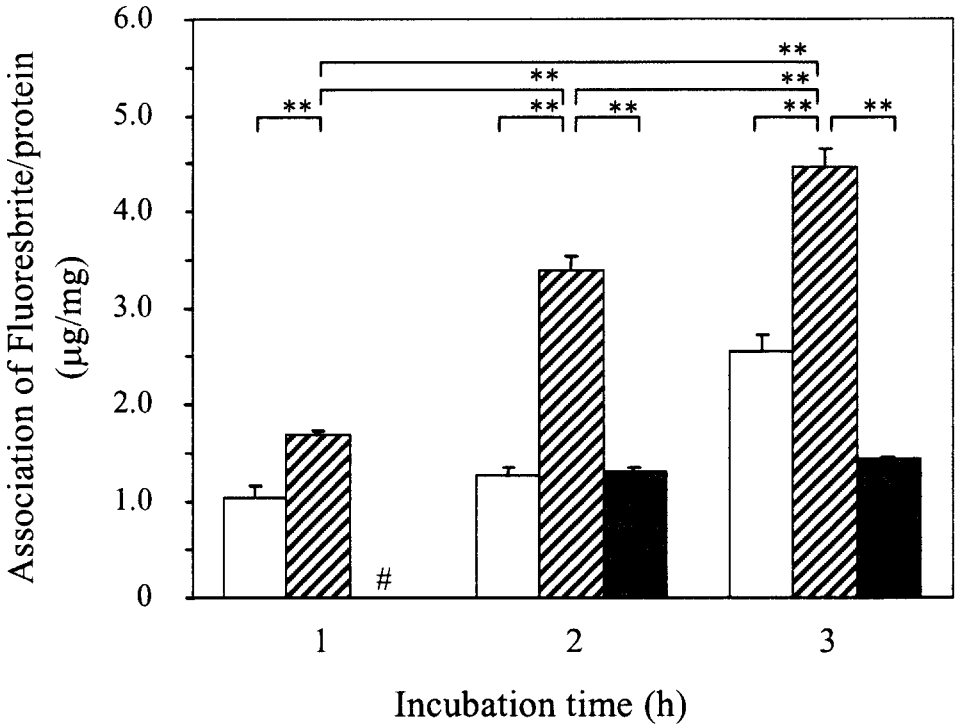

Figure 7. Association of Fluoresbrite entrapped in SG-liposomes with HepG2 cells

HepG2 cells (3×10^5 cells) were incubated with Fluoresbrite entrapped in SG-liposomes (100 μM as DPPC) for indicated times at 4°C (open bar) or at 37°C in the absence (hatched bar) or presence (closed bar) of 1 mg/mL AF.
Each value represents the mean±S.D. (n=3) #: Not determined, **:$p<0.01$, significantly different.

3.3. Association of DXR entrapped in SG-liposomes with HepG2 cells

To examine the interaction of SG-liposomes with HepG2 cells, the behavior of DXR entrapped in SG-liposomes was similarly examined. The association of DXR entrapped in SG-liposomes at 37°C increased with increasing incubation time (from 2 to 4 h, data not shown) and liposome concentration (from 0.1 to 1 mM as DPPC, data not shown). In Figure 8 the incorporation of DXR entrapped in SG-liposomes was compared with that entrapped in control liposomes. The effect of temperature and AF

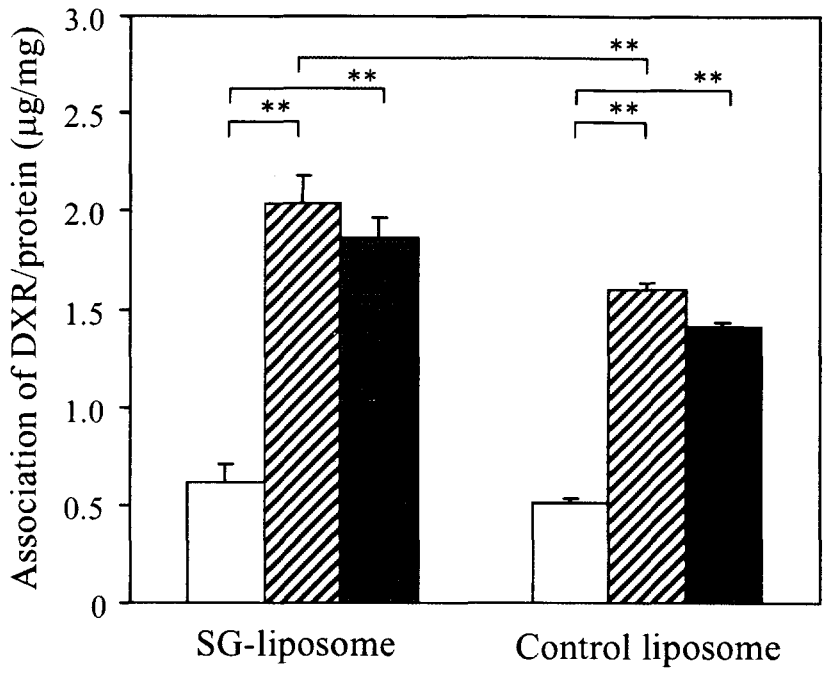

Figure 8. Association of DXR entrapped in SG- or control liposomes with HepG2 cells

HepG2 cells (3×10^5 cells) were incubated with DXR entrapped in SG-liposomes (100 μM as DPPC) for 4 h at 4°C (open bar) or at 37°C in the absence (hatched bar) or presence (closed bar) of 1 mg/mL AF. Control is liposome without SG.

Each value represents the mean±S.D. (n=3) **:$p<0.01$, significantly different.

on the association of DXR entrapped in SG-liposomes was examined after they were incubated for 4 h with HepG2 cells. The associated amount of DXR entrapped in SG-liposomes was higher when incubated at 37°C rather than 4°C. When DXR was applied as the SG-liposomal form, the amount of DXR associated with cells was increased four-fold with the incubation at 37°C than at 4°C (19.8% of that added at 37°C) and significantly higher than that of control liposomes ($p<0.01$). The association, however, was not affected by the addition of AF with SG-liposomes unlike in the case of DiI and Fluoresbrite.

About 20% of DXR was associated with HepG2 cells while 5.7% of

DXR appeared to be taken up *via* the AF sensitive pathway, when SG-liposomes (100 μM as DPPC) were incubated with HepG2 cells at 37°C. The greater part of DXR, which was accumulated in HepG2 cells, appeared to have been taken up as free DXR. To confirm the effect of free DXR on associated amount of total DXR, the associated amount of free DXR was compared with DXR entrapped in SG-liposomes, resulted in similar amount in both cases from 10 to 100 μg/mL DXR concentrations (data not shown). These findings corresponded well with the previous findings reported by Yachi et al. [49], in which the uptake of DXR entrapped in liposome, composed of dimyristoylphosphatidylglycerol/egg phosphatidylcholine/cholesterol *in vitro*, was equal to or lower than to that of free DXR incubated at 37°C, indicating that DXR in liposomes was taken up into the cells mainly after released from the liposomes. These findings raised the question of whether HepG2 cells took up the liposomes themselves or DXR after being released from the liposomes penetrated into the cells. Previously, it was demonstrated that SG-liposomes, liposomes containing SG, were unstable compared with liposomes containing cholesterol in terms of the high leakage of markers inside water pools in liposomes due to the high fluidity of the liposomal membrane at 37°C [50]. Because the leakage of aqueous phase markers entrapped in liposomes is enhanced by contact with cells [51], free DXR released from liposomes may influence the total association of DXR with cells. Therefore, the association of DXR entrapped in SG-liposomes was not affected by the addition of AF, since DXR released from SG-liposomes also accumulated into cells by its own properties, while a part of

SG-liposomes was taken up *via* the AF sensitive pathway.

In direct contact experiments *in vitro*, DXR entrapped in SG-liposomes and free DXR showed the same accumulation in HepG2 cells while *in vivo* [19] SG-liposomal DXR was much more efficient than free DXR. The discrepancy of DXR entrapped in SG-liposomes between *in vitro* and *in vivo* could describe as follows. In the case of *in vivo* situation, to reach the same drug concentration achieved with liposomal DXR in the liver, it would be necessary to administer a far higher dose of free DXR because of its wider tissue distribution. Some SG-liposomes that passed through the fenestration in the hepatic sinusoid could reach the surface of the hepatocytes, and were taken up as a liposomal form or free DXR released on or near the hepatocytes. Horowitz et al. [52] reported that the cytotoxic effect of DXR was mediated by the release of the drug from liposomes in the human ovarian carcinoma OV-1063 cell line. Therefore, released DXR from SG-liposomes may show high cytotoxic activity in the liver.

The accumulation of DXR entrapped in SG-liposomes in the liver[19] is described as follows (Figure 9). After intravenous injection, SG-liposomes prevent distribution of DXR to all organs as free DXR and deliver the drug near the site of action, i.e. the liver. SG-liposomes which could penetrate the fenestrae in liver would be taken up as a liposomal form *via* ASGP-R or AF sensitive way (Figure 9 (a)), or they released DXR near the hepatocyte by the interaction with cells (Figure 9 (b)).

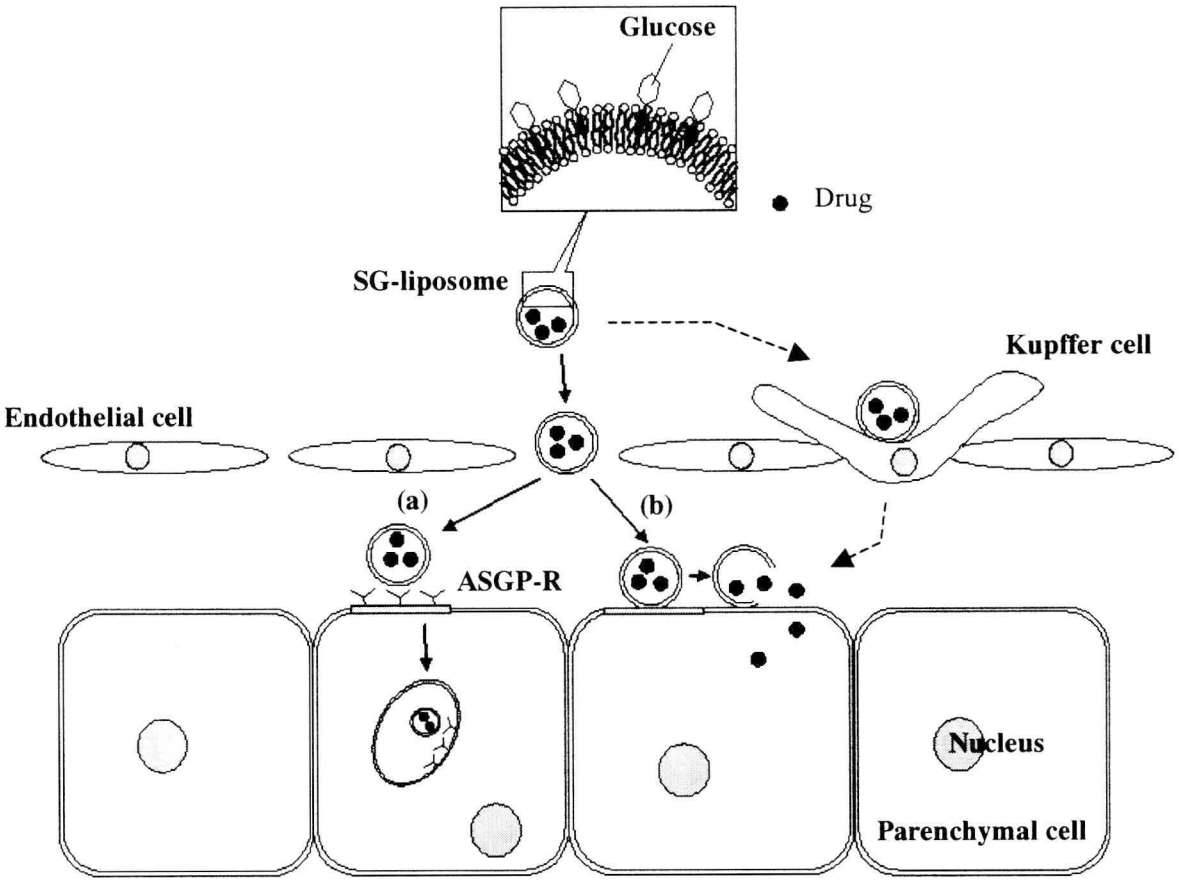

Figure 9. Schematic diagram of SG-liposomes entrapping DXR associated with HepG2 cells

(a) Receptor-mediated endocytosis pathway
(b) The accumulation of DXR after released from liposomes

4. Conclusions

The liver targeting efficiency of SG-liposomes was evaluated by means of measuring the associated amount of three different kinds of model drugs in HepG2 cells with emphasis on the involvement of ASGP-R mediated endocytosis, which recognizes galactose residue. The association of DiI (a lipophilic marker) and Fluoresbrite (a negative charged microsphere) were inhibited by the incubation with AF, while that of DXR was not affected by the addition of AF. These findings suggest that Fluoresbrite behaves like the lipid component of SG-liposomes, but DXR in SG-liposomes does not behave similar to the lipid component of SG-liposomes, thus, its drug behavior released from liposomes may be due to its physicochemical properties.

SG-liposomes are potentially useful drug carriers to the liver, because SG-liposomes have some interaction with hepatocytes *via* ASGP-R or at least AF-sensitive pathway.

CHAPTER 2

Penetration Enhancing Effect of β-Sitosterol Glucoside on Liver Cells

1. Introduction

As described in Chapter 1, SG-liposome is a potential drug carrier to the liver. In addition, SG and Sit-G, a major component of SG, have been reported as effective penetration enhancers of drugs across mucosal membranes and the enhancement effect of Sit-G is higher than that of SG[23,53]. Therefore, I examined whether Sit-G works as a penetration enhancer close to the hepatocyte.

Optical biosensor is a powerful technique to evaluate the interaction of biological macromolecules, such as protein-protein, drug-receptor and protein-cell interactions [54]. Without labeling of the absorbing species, it has ability to monitor the amount of adsorbed both continuously and exceedingly high sensitivity.

In this Chapter, the affinity of free Sit-G with HepG2 cells was measured using a resonant mirror optical biosensor (IAsys®). The penetration-enhancing effect of Sit-G on HepG2 cells was investigated by measuring the degree of association of FITC-dextran 4,400 (FD-4) with cells.

2. Experimental section

2.1. Materials

Sit-G was purchased from Essential Sterolin Products (Midrand, South Africa). FITC-dextran 4,400 (FD-4), Hank's balanced salt solution (HBSS) and dimethyl sulfoxide (DMSO) were purchased from Sigma Chemical Co. (St. Louis, MO, USA). Oleic acid (OA) was purchased from Tokyo Kasei Kogyo (Tokyo, Japan). RPMI 1640 medium, FBS and other materials used in cell culture were the same ones in Chapter 1. All other chemicals were of reagent grade.

2.2. Cell culture and cell preparation

Culture of HepG2 cells and its preparation for experiment were described in Experimental section of Chapter 1. For IAsys measurements, the cells were dispersed in PBS (consisting of 8.10 mM Na_2HPO_4, 1.47 mM KH_2PO_4, 137 mM NaCl and 2.68 mM KCl, pH 7.4) at appropriate concentrations.

2.3. IAsys measurements

Experiments were performed using an IAsys®, resonant mirror optical biosensor (Affinity Sensors, Cambridge, UK). Sit-G was immobilized on hydrophobic cuvette surfaces according to the manufacturer's instructions. A known concentration of HepG2 or HeLa cells was cumulatively added to the cuvette, and changes in resonant angle were monitored at 0.3-s intervals for approximately 22 min at 22°C.

2.4. Determination of cellular associated FD-4 by Sit-G

Sit-G or OA was dissolved into DMSO, and this solution was added to the 5 mg/mL FD-4 solution of HBSS to a final DMSO concentration of 1 %. HepG2 cells plated in 12-well tissue culture plates were incubated with FD-4 solution containing various concentrations of Sit-G for the indicated times at 4°C or 37°C. After incubation, cells were washed three times with ice-cold HBSS and dissolved in PBS containing 0.2% Triton X-100.

Associated amount of FD-4 was measured using a fluorophotometer (Hitachi F-4010, Tokyo, Japan) with excitation and emission wavelengths of 490 and 520 nm, respectively. That of Sit-G was determined by HPLC. The HPLC system was the same as described in Chapter 1, with SPD-6A UV spectrophotometric detector. The cell lysate was dried under a gentle N_2 gas stream (at 60°C) and redissolved in methanol. The sample solution was injected into the column (Nova-Pack C18, Waters) and detected at 210 nm. Elution was carried out at 40°C with methanol as the mobile phase at a flow rate of 1.0 mL/min.

The cell protein was measured using a BCA protein assay kit and the results are presented as associated amount of FD-4 or Sit-G per mg of cellular protein.

2.5. Statistical analysis

Data were compared using analysis of variance and Student's *t*-test. A *p*-value of 0.05 or 0.01 was considered significant.

3. Results and Discussion

3.1. Affinity of Sit-G with HepG2 cells

The affinity of SG-liposomes to HepG2 cells was shown in Chapter 1, however, it may imply other interactions. It is difficult to divide ASGP-R mediated endocytosis and penetration-enhancing effect of SG-liposomes since they occurred only at 37°C. Therefore, I assessed the interaction between Sit-G and HepG2 cells in real time using the IAsys® cuvette-based resonant mirror system. The adsorption of material onto the horizontal sensor surface is followed by resonance angle shifts, provided the adsorbed material has a refractive index different from that of the bulk solution. The biosensor measures changes in resonant angle that occur on binding of HepG2 or HeLa cells to Sit-G immobilized on a cuvette surface in real time.

Figure 10 shows sequential binding of the cells with Sit-G when the cells were cumulatively added to the cuvette. Interaction of Sit-G with both cell lines was increased with time and cell concentration, and changes in HepG2 cells were obvious compared to those in HeLa cells. These observations suggested that Sit-G has higher affinity with HepG2 than HeLa cells. This affinity might be one of reasons for accumulation of SG-liposomes in the liver.

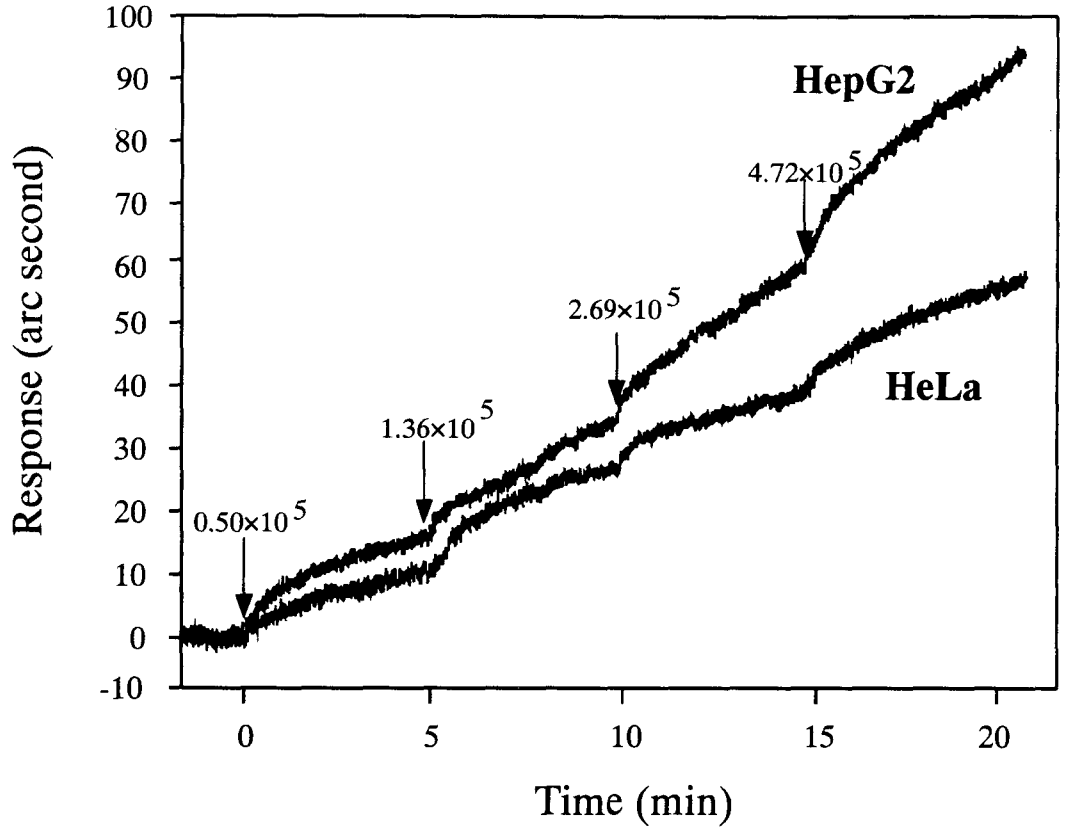

Figure 10. IAsys interaction profile of HepG2 and HeLa cells with Sit-G
Arrows indicate addition of HepG2 or HeLa cells to the final concentrations shown (cells/mL).

3.2. Penetration-enhancing effect of Sit-G in hepatocytes

SG and Sit-G have been reported to be penetration enhancers and Sit-G was a more effective enhancer than SG [23, 53]. When SG-liposomes accumulated in the liver, the concentration of Sit-G might be the level leading penetration-enhancing effect close to hepatocytes. To estimate the penetration-enhancing effect of Sit-G in hepatocytes, 5 mg/mL FD-4 solution was incubated with HepG2 cells in the presence of 100 μM OA or Sit-G for 1 h at 4°C or 37°C as shown in Figure 11. FD-4 is one of suitable model drug to see the penetration-enhancing effect. The FD-4

solution used in these experiments contained 1% DMSO to disperse these enhancers uniformly because of their fairly low solubility in water. OA was used as an active control as it is often used as a penetration enhancer by increasing the motional freedom or fluidity of membrane phospholipids[55], and is capable of nonspecific disruption of the alveolar membrane at high concentrations (0.1 mM) [55,56]. The association of FD-4 was not enhanced by 100 μM OA at 37°C, showing the same value as at 4°C and control (FD-4 solution containing 1% DMSO), but Sit-G (100 μM) significantly increased it at 37°C as compared that with at 4°C. These findings suggested that Sit-G increased the association of FD-4 with HepG2 cells at 37°C.

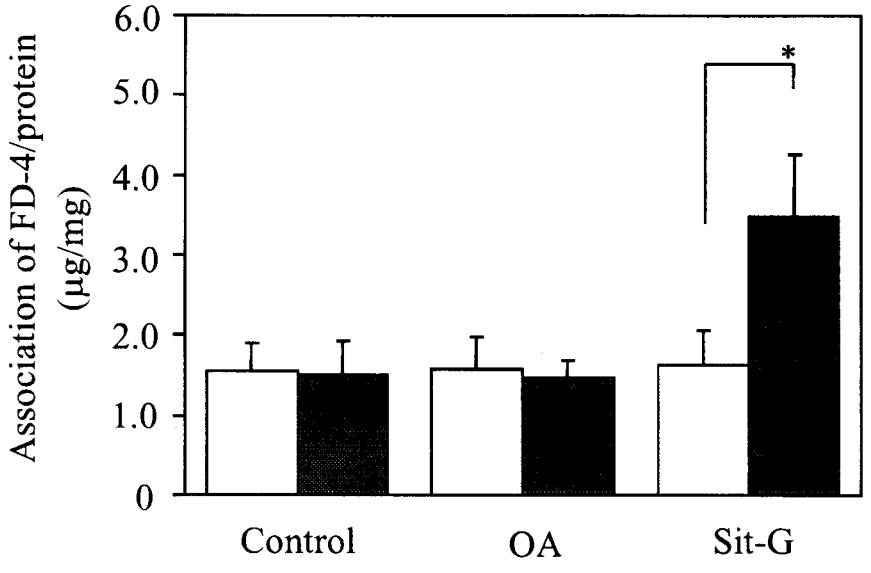

Figure 11. Association of FD-4 with HepG2 cells after incubation of 5 mg/mL FD-4 solution containing 1% DMSO with 100 μM OA or 100 μM Sit-G for 1 h at 4°C (open bar) or 37°C (closed bar)

As a control, 5 mg/mL FD-4 solution containing 1% DMSO was applied.
Each value represents the mean ± S.D. (n=3-4) *: $p<0.05$

Effects of Sit-G concentration on the association of both FD-4 (Figure 12 (a)) and Sit-G (Figure 12 (b)) incubated with 5 mg/mL FD-4 solution were examined for 1 h with HepG2 cells. The levels of association of FD-4 and Sit-G at 37°C were increased with increases in Sit-G concentration and positive correlations were found between the amounts of FD-4 and Sit-G (r=0.964 between association of FD-4 and Sit-G).

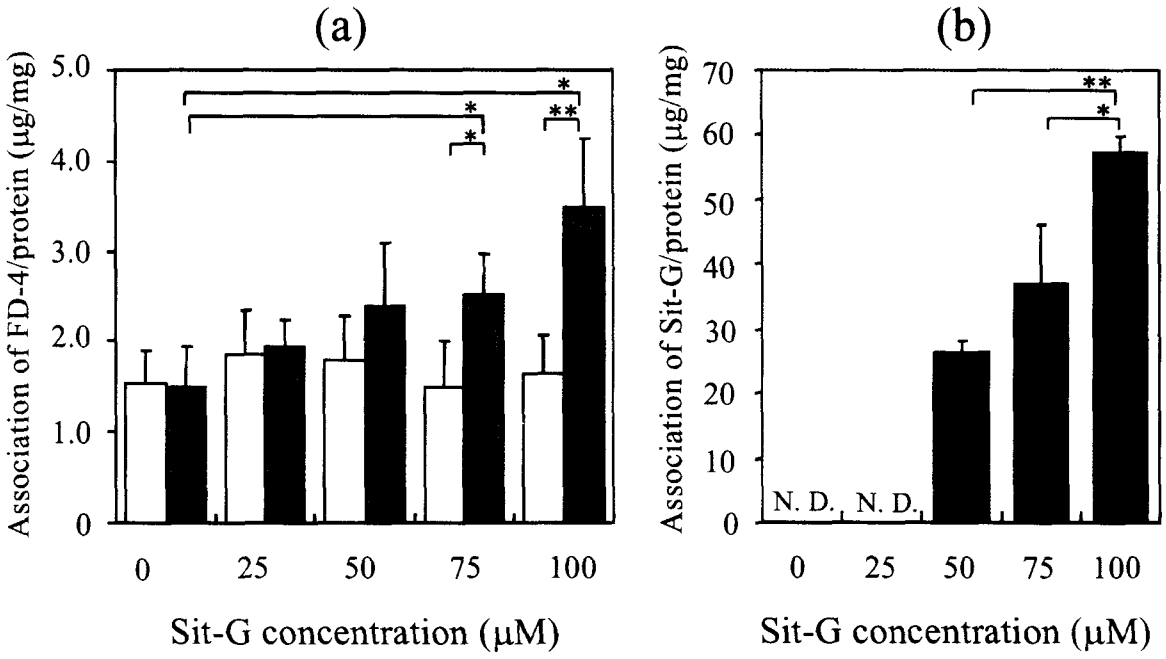

Figure 12. Effects of Sit-G concentration on the association of FD-4 (a) and Sit-G (b) with HepG2 cells incubated at 4°C (open bar) or 37°C (closed bar) for 1 h

Each value represents the mean ± S.D. (n=3-4) *: $p<0.05$, **: $p<0.01$, N. D.: not detected

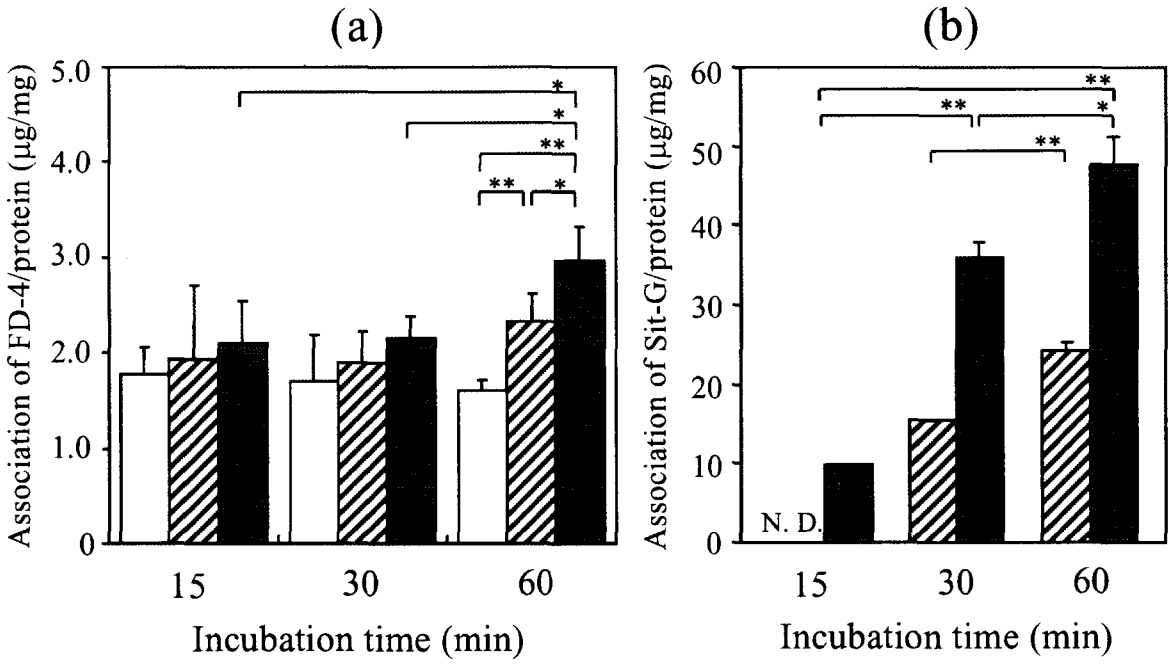

Figure 13. Effects of incubation time on the association of FD-4 (a) and Sit-G (b) with HepG2 cells incubated with 50 μM (hatched bar) and 100 μM (closed bar) and without (open bar) Sit-G at 37°C

Each value represents the mean ± S.D. (n=3-4)
*: $p<0.05$, **: $p<0.01$, N. D.: not detected

The effects of incubation time on the association of FD-4 (Figure 13 (a)) and Sit-G (Figure 13 (b)) with HepG2 cells incubated in FD-4 solution containing 50 or 100 μM Sit-G at 37°C were examined. The association of FD-4 without Sit-G did not increase during the incubation period, but at higher concentrations of Sit-G the level of association of FD-4 and Sit-G increased with incubation time.

The effects of incubation time and Sit-G concentration on the association % of FD-4 and Sit-G are summarized in Table 4. The association % of Sit-G was approximately 10 % of that added after 60 min incubation regardless of Sit-G concentration added, suggesting

partitioning of Sit-G into the cell membrane. These results suggested that Sit-G increases the association of FD-4 by means of distribution of Sit-G into the cell membrane. Following application of FD-4 powder containing Sit-G (FD-4/Sit-G=1/2, w/w) to excised rabbit nasal mucosa for 30 min *in vitro*, incorporation of 3.3 % Sit-G into the nasal mucosa increased FD-4 permeability by approximately 1.8-fold compared to the control [57]. These findings confirmed that Sit-G is a mucosal penetration enhancer [23, 53] and enhances the permeability by increasing the fluidity of phospholipid membranes [23].

Table 4. Effects of incubation time and Sit-G concentration on the association % of FD-4 and Sit-G incubated with HepG2 cells at 37°C

Incubation time (min)	Sit-G conc. (μM)	Association % of added	
		FD-4 ($\times 10^{-3}$)	Sit-G
15	0	3.88 ± 0.93	- [a]
	50	4.79 ± 1.85	- [a]
	100	6.48 ± 1.36	2.20 ± 0.19
30	0	4.03 ± 1.04	- [a]
	50	4.14 ± 0.95	5.84 ± 0.56
	100	4.97 ± 0.81	7.18 ± 1.05
60	0	2.71 ± 0.19	- [a]
	25	3.86 ± 0.54	- [a]
	50	5.12 ± 1.05	9.86 ± 0.89
	75	5.54 ± 1.32	9.15 ± 2.09
	100	7.65 ± 1.16	11.68 ± 1.03

[a] : Not detected

Each value represents the mean ± S.D. (n=3-4).

4. Conclusions

IAsys measurement elucidated that the Sit-G had an affinity with HepG2 cells. The association of FD-4 with HepG2 cells was increased by the incubation with Sit-G. Therefore, Sit-G, which may be released from Kupffer cells after degradation of SG-liposomes, would increase the association of drug. Taking these observations into consideration, SG-liposomes are not only liver targeting drug carrier, but also enhance the penetration of drugs near the hepatocyte. These results indicated that Sit-G may exhibit a property as both a ligand for liver targeting and a penetration enhancement near hepatocytes.

CHAPTER 3

Preparation and Pharmacokinetics of Sit-G-liposomes Entrapping Pirarubicin

1. Introduction

Pirarubucin (THP) is a DXR derivative which has higher antitumor effect with lower adverse effect than DXR. However, the THP level in the liver was low after intravenous administration of THP solution compared with that of DXR [58]. THP is utilized for intra-arterial or intraportal administration and for chemoembolization of lipiodol emulsion instead of DXR on liver metastasis and hepatocellular carcinoma [59-61].

As discussed in Chapters 1 and 2, SG-liposomes are potential drug carrier to liver and Sit-G has possibility to increase the drug accumulation in hepatocyte. Therefore, THP entrapped in SG-liposomes could enhance the therapeutic efficacy of liver tumors. However, there are no studies about liposomal THP to my knowledge.

The high entrapment of drugs into small sized liposomes by passive loading method is not high enough, and the pH gradients method that lead quantitative drug loading of vesicles through inward active drug diffusion are limited to drugs of small molecular weight, appropriate lipophilicity and certain structural characteristics [62]. The dehydration-rehydration vesicle (DRV) method [34] can entrap the drugs regardless of the molecular size and other characteristics such as carboxyfluorescein, albumin and DNA, but the size of liposomes was the relatively large, in some cases reaching micrometer size. Therefore, to prepare small sized liposomes with high entrapment efficiency of THP, I selected the DRV method as reported by Zadi et al. [63] with some modifications. In the modified DRV method, the dehydration of a mixture of empty small

unilamellar vesicles (SUV) and drug destined for entrapment is carried out in the presence of sugars on the external side of liposomes i.e., sugars help more drug entry into the vesicles and prevents larger vesicle formation. This method was applied to DXR, but not THP and no *in vivo* studies were reported.

In this Chapter, THP-entrapping Sit-G-liposomes (L-THP) were prepared and evaluated their pharmacokinetics and antitumor effects against the liver metastasis of M5076 in mice.

2. Experimental section

2.1. Materials

THP hydrochloride for injection was supplied by Nippon Kayaku Co. Ltd. (Tokyo, Japan). Purified yolk lecithin (EPC) was supplied by Q.P. Co. (Tokyo, Japan). Cholesterol, Sit-G and OA was same as described in Materials of Chapter 1 and 2. Sucrose was purchased from Wako Pure Chemical Industries Ltd., (Osaka, Japan). Chemicals for HPLC were of HPLC grade and, all other chemicals were of analytical grade.

2.2. Animals and tumor cells

Specific-pathogen-free female C57BL/6j mice (17-19g) were purchased from Tokyo Laboratory Animals Science Co., Ltd. (Tokyo, Japan). Murine histiocytoma M5076 cells were supplied by the Cancer Chemotherapy Center of the Japanese Foundation for Cancer Research (Tokyo, Japan). After 4 transplant generations, the tumor cells were used in this study. The cells were kept as a solid tumor in C57BL/6j mice and transplanted every three weeks. The experimental procedures were performed according to the rules set by the Committee on Ethics in the Care and Use of Laboratory Animal in Hoshi University.

2.3. Preparation of L-THP

Liposomal THP (L-THP) was prepared from EPC, Ch, Sit-G and OA (EPC:Ch:Sit-G:OA=7:3:2:0~3, in molar ratio) by DRV method with some modification (Figure 14). All lipids were dissolved in a chloroform-

methanol mixture (1:1) and the solvent was evaporated. The dried lipid mixture was hydrated with distilled water to form multilamellar vesicles (MLV), that were changed to small unilamellar vesicles (SUV) (average particle size, about 80-100 nm) by sonication using an ultrasonic disruptor (TOMY UD-200, Tomy Seiko Co., Ltd., Tokyo, Japan). The pH value of SUV suspensions was adjusted at 7.4 by 0.1 M NaOH solution to prevent the aggregation of SUV after mixing with THP. THP and sugars (glucose, lactose or sucrose) were mixed with the SUV suspensions at each

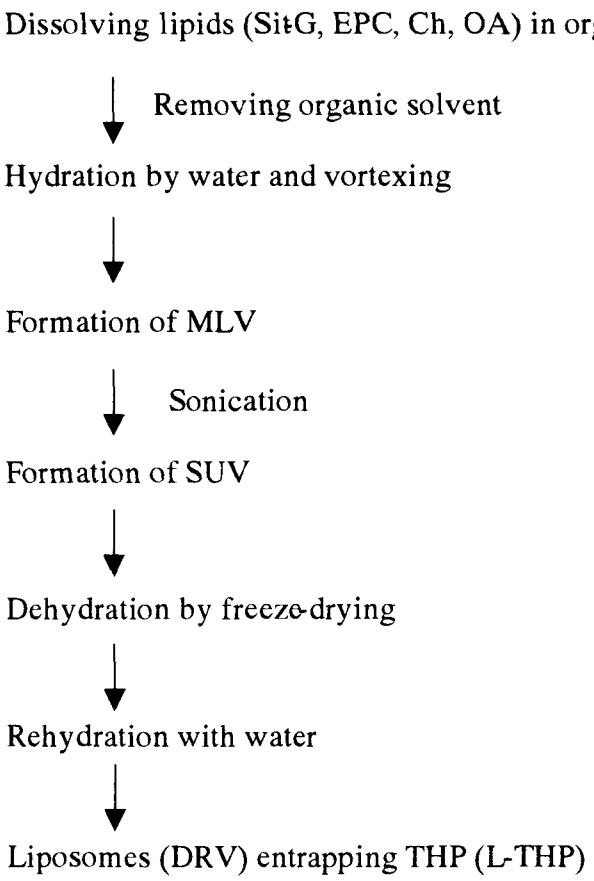

Figure 14. Preparation of liposomes entrapping THP by DRV method

indicated weight ratio. The resulting mixtures were then freeze-dried overnight. The powders obtained after freeze-drying were rehydrated with water in a manner similar to that applied in the DRV technology [34,64]. Finally, the concentration of THP in liposome suspensions was adjusted to 0.5 mg/mL.

2.4. Measurement of size, entrapment efficiency and micrographs of L-THP

The average particle size of liposomes was determined using a dynamic laser light scattering instrument (ELS-800, Ostuka Electronics Co., Ltd., Osaka, Japan). Entrapment efficiency of THP was calculated from the THP concentration of supernatant (C_f) after separation of 1/20 diluted L-THP suspension by ultracentrifugation (100,000 ×g, 60 min, 4°C) determining by fluorescent spectrometer (Hitachi F-4010, Tokyo, Japan) at 482 nm for excitation and 550 nm for emission, $(1- C_f / C_{total}) \times 100$ (%), where C_{total} is the THP concentration of total liposome suspension. The shape of liposomes before and after rehydration was observed using the scanning electron microscope (JSM-5600LV, JEOL Co. Ltd., Tokyo, Japan).

2.5. Biodistribution of L-THP

The solid tumors of M5076 were dispersed with sterile saline by gentle homogenization on the mesh and this suspension was injected on day 0 *via* the tail vein (1×10^5 cells/animal). At 14 days after tumor inoculation, the metastatic tumor nodules were observed mainly in liver

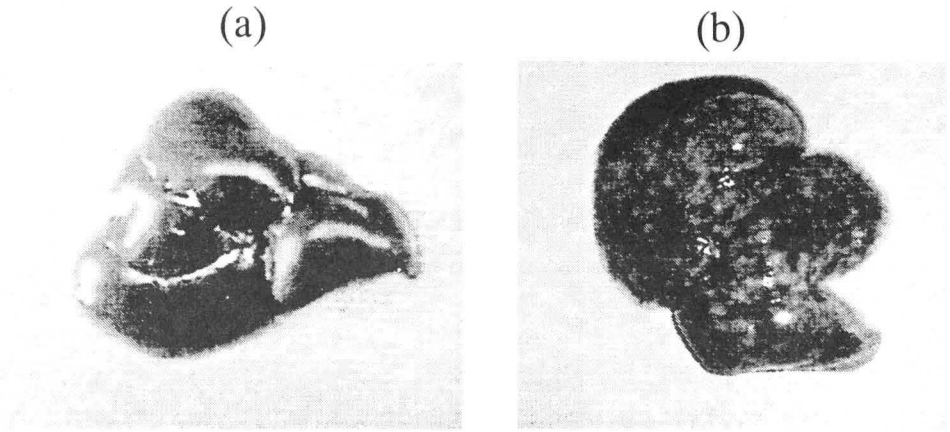

Figure 15 Pictures of the liver

(a) Healthy liver

(b) At 14 days after M5076 tumor inoculation

(Figure 15). L-THP (EPC:Ch:Sit-G:OA=7:3:2:1, molar ratio) with sucrose to total lipid weight ratio at 8, which was almost isotonic solution, was used. Free THP (F-THP) was THP solution of 5% glucose (0.5 mg/mL). At 10 days after M5076 cells inoculation, the mice were injected F-THP or L-THP at a dose of 5 mg/kg intravenously. Four mice were used at each predetermined time after i.v. injection (0.5, 1, 2, 6, 24 h) and blood and their tissues (heart, lung, liver, kidney and spleen) were collected. The concentration of THP in serum and tissues was measured by the HPLC assay method [65, 66]. The HPLC system was composed of an LC-10AS pump (Shimadzu Co., Japan), a SIL-10A autoinjector (Shimadzu Co., Japan), a RF-10A_{XL} fluorescence detector (Ex, 482 nm, Em, 550 nm, Shimadzu Co., Japan) and a YMC-Pack ODS-A, 150×4.6 mm I. D. column (YMC Co., Ltd., Japan). The mobile phase was 0.1 M ammonium formate (pH 4.0): acetonitrile =7:3 (v/v) and the flow rate was 1.0 mL/min. The

concentration of THP in each sample was determined using a calibration curve, using daunomycin as the internal standard. Pharmacokinetic parameters for THP in serum were estimated by the nonlinear least squares program (MULTI) [67]. The areas under the biodistribution curves (from 0 h to 24 h) ($AUC_{0\text{-}24}$) of THP in tissues were calculated using the trapezoid method. Statistical comparison was performed using the Bonferroni/Dunn post-hoc test with $p<0.05$ indicative of significance.

2.6. Antitumor experiment

M5076 cells were injected on day 0 *via* the tail vein (1×10^5 cells/animal). The treatment of F-THP or L-THP started on the day 3, was injected intravenously at a dose of 10 mg/kg. The control group was injected with the same volume of sterile 5% glucose solution. Antitumor effects were determined by comparing the mean survival time of treated groups (T) with that of control group (C) and expressed as an increase in life span (ILS), ILS=(T/C-1) ×100 (%). For the survival test, Kaplan-Meier curves were constructed and the survival ratios were compared by the log-rank test. Differences were considered significant when the *p*-value was less than 0.05.

3. Results and Discussion

3.1. Preparation of L-THP by DRV method

To deliver drugs to the liver using liposomes, it is important to control the particle size under about 400 nm to evade uptake by the reticuloendothelial system and also to maintain a high entrapment efficiency of the drugs. Usually, it is very difficult to entrap drugs highly in small-sized liposomes. The active entrapment method using a transmembrane pH gradient failed to entrap THP probably because of its low solubility in the buffer solution. Therefore, I selected the modified DRV method to prepare liposomal THP. In this method, the particle size of liposomes and the entrapment efficiency of drugs are influenced by the kinds of sugars and the ratio of the drugs, sugars and OA to lipids in liposomes. I fixed the THP/EPC ratio at 0.05 (w/w), because at the higher ratio of THP (THP/EPC=0.1 (w/w)), the rehydrated liposomes consisting of EPC:Ch:Sit-G:OA=7:3:2:1 became 1254.9 ± 223.5 nm while those at THP/EPC=0.05 was 341.0 ± 41.1 nm (data not shown).

3.2. The effect of sugars and OA on the particle size and entrapment efficiency of L-THP

First of all, I confirmed the effect of sugars on the average particle size and the THP entrapment of L-THP with or without OA as shown in Table 5. Three kinds of sugars were tested, i.e., glucose, sucrose and lactose when the mass ratio of sugar to total lipid was 1. In both liposomes prepared without sugar, the average particle size was

significantly larger (greater than 1,000 nm), whereas with sugar it was small. The particle sizes of L-THP (7:3:2:1) with glucose and sucrose were 675.5 nm and 768.1 nm, respectively. The effect of sucrose and glucose was almost equal and greater than that of lactose. Since it has been reported that sucrose, i.e., disaccharide is effective to prevent fusion than glucose, i.e., monosaccharide [63, 68], sucrose was selected as sugars.

The entrapment efficiency of L-THP without OA was 31-35% regardless of with or without sugar, but that with OA was 78-87%. Incorporation of negatively charged lipid, i.e. OA, into liposomes increased the retention of positively charged THP in liposomes and, therefore, the particle size was increased.

To determine the optimal ratio of sucrose to lipids, the ratio of sucrose to lipid was examined. When increasing the amount of sucrose,

Table 5. The effect of sugars on the average particle size and entrapment efficiency of L-THP at sugar:lipid=1:1 (w/w)

Molar ratio (EPC:Ch:Sit-G:OA)	Sugar	Average particle size (nm)	Entrapment efficiency (%)
L-THP (7:3:2:0)	Without sugar	1113.7 ± 146.3	31.7± 1.3
	Glucose	187.3 ± 6.1	31.4± 4.2
	Lactose	389.5 ± 18.1	33.8± 2.9
	Sucrose	147.2 ± 0.9	35.0± 0.1
L-THP (7:3:2:1)	Without sugar	1510.3 ± 52.3	84.8± 8.0
	Glucose	675.5 ± 72.8	87.0± 0.4
	Lactose	1245.4 ± 236.7	77.7± 1.1
	Sucrose	768.1 ± 102.7	83.9± 8.7

THP/EPC=0.05 (w/w)
Each value represents the mean ± S.D. (n=3).

the increasing average particle size after the dehydration-rehydration steps was moderately inhibited without reduction of entrapment efficiency (Table 6). At the 8:1 ratio of sucrose to lipid, the smallest vesicle with high entrapment efficiency was obtained.

The effect of OA on the particle size of liposomes and the entrapment efficiency is shown in Figure 16. The entrapment efficiency was increased with increase of OA ratio in liposomes (EPC:Ch:Sit-G:OA=7:3:2:1~3 in molar ratio, THP/EPC=0.05 in weight and sucrose:total lipid=8:1 in weight), but the particle size was also increased, perhaps because of interaction of THP with OA. From these results, L-THP (EPC:Ch:Sit-G:OA=7:3:2:1 in molar ratio) prepared with THP/EPC=0.05 in weight had less than 400 nm particle size (size about 340 nm) with higher entrapment efficiency (about 80%), therefore, this L-THP (7:3:2:1) with a sucrose to lipid ratio of 8:1 was used for the animal experiments.

Table 6. The effect of the sucrose to lipid ratio on the average particle size and entrapment efficiency of L-THP

Molar ratio (EPC:Ch:Sit-G:OA)	Sucrose/ lipid (w/w)	Average particle size (nm)	Entrapment efficiency (%)
L-THP (7: 3: 2: 1)	0	1510.3 ± 52.3	84.8 ± 8.0
	1	768.1 ± 129.6	83.9 ± 8.7
	2	423.7 ± 35.8	82.4 ± 10.7
	5	412.4 ± 1.5	82.6 ± 4.9
	8	341.0 ± 41.1	80.7 ± 11.3

THP/EPC=0.05 (w/w)

Each value represents the mean ± S.D. (n=3).

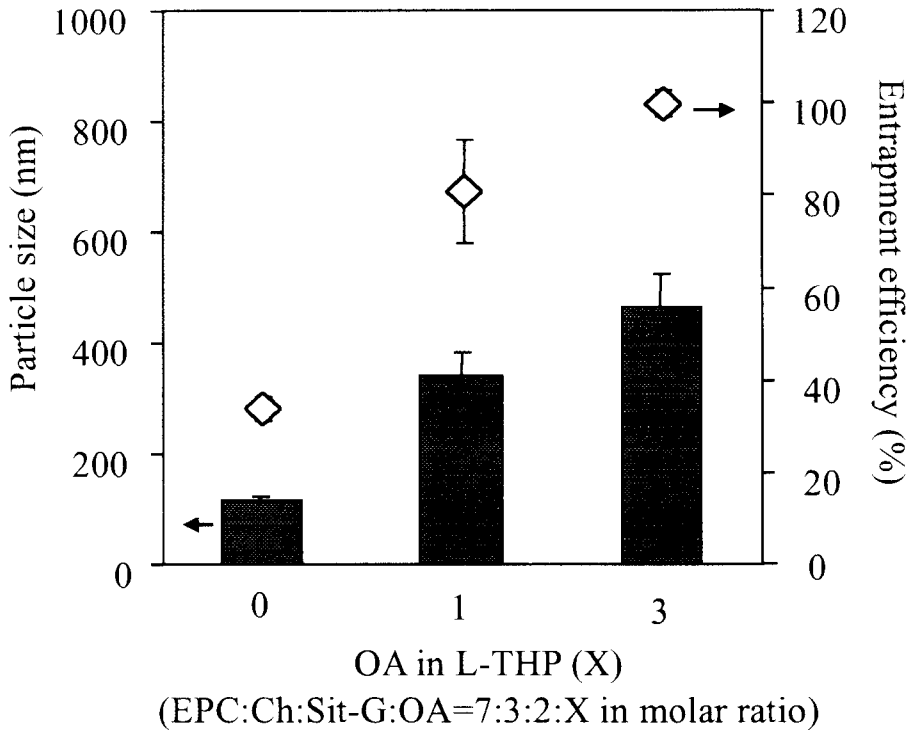

Figure 16. The effect of OA ratio in L-THP on the particle size of liposomes (bar) and the entrapment efficiency (◇)

L-THP was prepared from EPC:Ch:Sit-G:OA=7:3:2:X (molar ratio) at sucrose:lipid=8:1 (w/w) and THP/EPC=0.05.
Each value represents the mean ± S.D. (n=3).

3.3. The scanning electron micrograph of L-THP

To confirm the liposome structure in each preparation stage, the scanning electron micrographs of L-THP (7:3:2:1) were taken (Figure 17). Under the lyophilized state with sucrose, liposomes appeared to be buried in a glassy matrix of sucrose (Figure 17 (a)). Lyophilization without sucrose led liposomes aggregating completely (data not shown), and resulted in larger vesicles (greater than 1,000 nm) after rehydration. After rehydration of lyophilized L-THP (7:3:2:1) with sucrose, small vesicles were reconstructed (Figure 17 (b)).

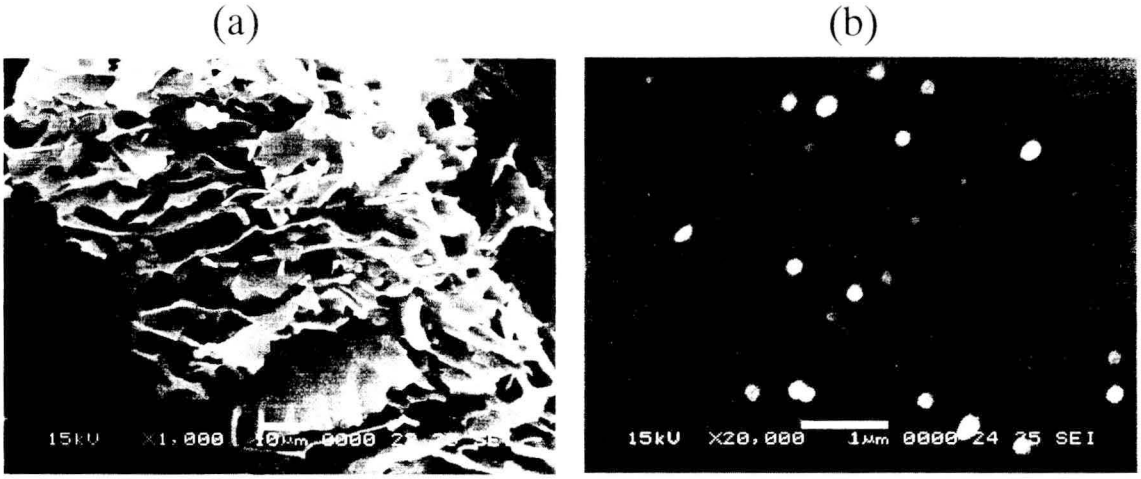

Figure 17. Scanning electron micrographs of L-THP before (a) and after (b) rehydration

L-THP was prepared from EPC:Ch:Sit-G:OA=7:3:2:1 (molar ratio) at sucrose:lipid=8:1 (w/w).

3.4. Pharmacokinetics and antitumor effects of L-THP

The pharmacokinetics and antitumor effects of L-THP (EPC:Ch:Sit-G:OA= 7:3:2:1 in the molar ratio and sucrose:total lipid = 8:1 in weight) are evaluated in mice bearing liver metastasis of M5076 cells. Murine histiocytoma M5076, which arises spontaneously in mice ovaries[69], is highly invasive and metastasizes to several organs including the liver and spleen [70].

The serum and tissue $AUC_{0\text{-}24}$ values calculated from the biodistribution curves of F-THP and L-THP are shown in Table 7. F-THP accumulated highly in lung and spleen, which correspond well with Iguchi et al. [58] and Fujita et al. [71]. L-THP changed the biodistribution of THP, i.e., increasing the $AUC_{0\text{-}24}$ value of liver and decreasing those of heart,

lung, kidney and spleen. The AUC_{0-24} value of L-THP in the liver (24.4 μg·h/g), where the tumor represented, was approximately 4-fold that of F-THP (6.6 μg·h/g). The drug accumulation in the heart correlated to the cardiotoxicity. THP is less cardiotoxic than DXR, because the accumulation of THP in the heart was lower than that of DXR [19, 58]. L-THP significantly decreased the AUC value in the heart (3.7 μg·h/g) compared with that of F-THP (7.7 μg·h/g), suggesting that L-THP is safer than F-THP.

After administration at a dose of 10 mg/kg, the mice treated both F-THP and L-THP prolonged the median survival time than control and the ILS values of F-THP and L-THP were 28.6 and 42.9%, respectively (Table 8). L-THP did not decrease largely the body weight of mice unlike F-THP that decreased to about 10% of the initial body weight (data not shown), reflecting an adverse effect. No lethal toxicity was observed in C57BL/6j mice treated with THP up to 15 mg/kg (data not shown), while it was reported that the LD_{50} value is 14.1 mg/kg in female ddY mice [72].

Table 7 Tissue AUC_{0-24} values after injection of F-THP and L-THP in mice bearing M5076 at a dose of 5 mg/kg at 10 days after tumor inoculation (n=4)

	Tissue AUC_{0-24} (μg·h /g)					
	Serum [a]	Liver	Heart	Lung	Kidney	Spleen
F-THP	1.13	6.6 (0.8)	7.7 (1.0)	485.1(179.5)	90.2 (50.5)	130.7 (24.4)
L-THP	1.45	24.4* (3.2)	3.7* (0.9)	93.0* (4.3)	24.0* (1.8)	101.3 (20.9)

[a] Serum AUC is given as μg · h /mL. The numbers in parentheses represent S.D.
*: $p<0.05$, compared with F-THP

This finding suggested that L-THP kept equal or superior antitumor effect to F-THP on M5076 liver metastasis with less adverse effects. Systemic injection of L-THP is a potential treatment for liver cancer, because the liposomes can safely carry THP to the liver.

Table 8. Antitumor effects of F-THP and L-THP in mice bearing M5076 liver metastasis tumors treated at 10 mg/kg at 3 days following tumor inoculation (n=7)

	Median survival time (days)	ILS [a] (%)
Control	14.0	
F-THP	18.0	28.6 *
L-THP [b]	20.0	42.9 *

[a] Percentage increase in life span, (T/C-1) × 100 (%), where T and C represent the median survival time of the treated and control animals, respectively. [b] L-THP consisted of EPC:Ch:Sit-G:OA=7:3:2:1 (molar ratio).

*: $p<0.05$, compared with control

4. Conclusions

Using the modified DRV method, small sized liposomes highly entrapping THP were obtained by the addition of OA into a formulation (EPC:Ch:Sit-G:OA=7:3:2:1 in molar ratio), and by the addition of sucrose in preparations. L-THP increased the accumulation of THP in the liver, and had potential antitumor effects than F-THP in M5076 tumor bearing mice. A novel potential application of THP in liver tumors was found by the liposome dosage form.

SUMMARY

Cancer chemotherapy with anticancer drugs is not regarded as an effective treatment, because their narrow therapeutic window causes intolerable toxicity, such as alopecia, cardiotoxicity, bone marrow suppression and gastrointestinal disorder, which would decrease the quality of life of patients. Therefore, delivery of anticancer drugs to tumor site is required for efficient drug treatment. For this purpose, particulate drug carriers are utilized for selective drug delivery to cancer.

DXR is widely used antitumor drug and is clinically used for the liver cancer treatment although the severe adverse effect is an obstacle. To increase the therapeutic efficacy of DXR in liver cancer, liposomes modified with SG, which is a ligand to the liver (SG-liposomes), were used. SG-liposomes carried DXR to the liver effectively, and increased antitumor effects in mice bearing M5076 metastatic liver tumor. However, the mechanism of SG-liposomes to liver targeting is not clear.

In this thesis the effect of SG-liposomes or liposomes modified with Sit-G, which is a main component of SG, (Sit-G-liposomes) as a drug carrier to the liver was evaluated. Furthermore, THP having higher lipophilicity than DXR was selected for the liver cancer treatment and entrapped in Sit-G-liposomes. THP entrapped Sit-G-liposomes (L-THP) were prepared and evaluated their pharmacokinetics and antitumor effects.

In Chapter 1, the efficiency of SG-liposomes as a drug carrier to the liver was estimated in HepG2 cells with emphases on the ASGP-R.

The association of DXR or two different kinds of marker (DiI and Fluoresbrite) entrapped in SG-liposomes indicated that liposomal membrane itself and Fluoresbrite were taken up *via* ASGP-R or AF sensitive pathway. However, the effect of SG-liposomes on DXR accumulation was not evaluated clearly, because free DXR released from liposomes was easily taken up to the cells.

SG and Sit-G have been reported as a penetration enhancer. After intravenous administration, particulate drug carriers, which are larger than 400 nm, tend to be clear by macrophages in the liver and spleen (RES). Therefore, the released SG or Sit-G from macrophages after degradation of liposomes might increase the association of drugs delivered by SG-liposomes with cells as an enhancer. In Chapter 2, the affinity and penetration-enhancing effect of Sit-G was evaluated. Some affinity or interaction of Sit-G with HepG2 cells was observed. After incubation with FD-4 (model drug) and Sit-G, the association of FD-4 and Sit-G with HepG2 cells was proportionally increased with concentration of Sit-G, indicating that the Sit-G may perturb the cell membranes by incorporating in it and then enhance the penetration of FD-4. From these results, SG-liposomes are potentially useful drug carriers to the liver, because SG interacts with hepatocytes *via* ASGP-R (Figure 18 (a)), and may increase the penetration of drugs carried by liposomes near the hepatocytes (Figure 18 (b)).

THP shows faster cellular uptake and has higher antitumor effect than DXR. L-THP was prepared to increase the antitumor effect of THP in liver cancer. To prepare the high entrapment of THP in small sized

liposomes, OA was added in a formulation and sucrose was used in DRV preparation method. THP from L-THP accumulated in the liver and prolonged the survival time of mice bearing liver metastasis tumor without body weight loss unlike free THP. L-THP is a novel potential dosage form of THP in liver tumors.

In conclusion, liposomes modified with SG and Sit-G provides usefulness as potential drug carrier to the liver, because SG and Sit-G work as a liver targeting and a penetration enhancer. They may give new opportunities of liver disease treatment for conventional drugs which are not sufficiently effective or which display serious side effects.

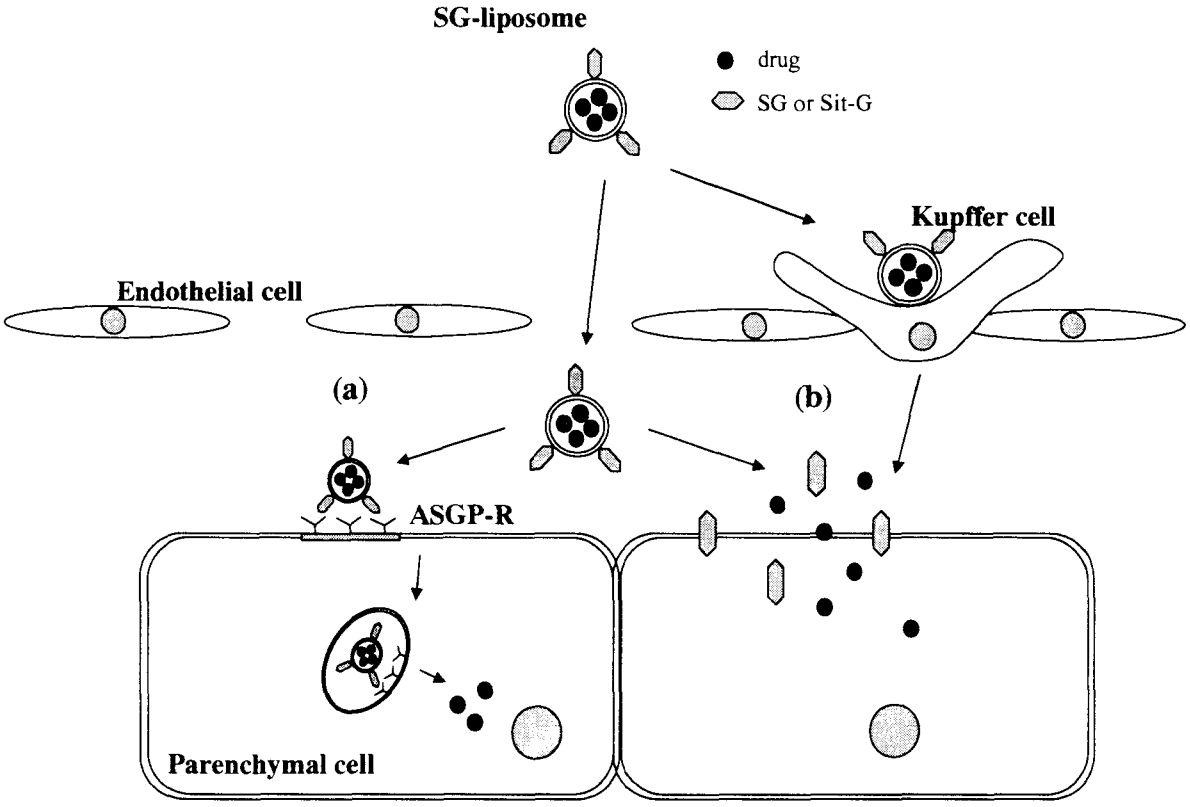

Figure 18. Schematic diagram of SG-liposomes entrapped DXR associated with HepG2 cells

ACKNOWLEDGEMENTS

First, I would like to express my gratitude and appreciation from my heart to Professor Yoshie Maitani for helpful guidance in my research work and preparing this dissertation.

Further, I wish to thank Professor Kozo Takayama and Emeritus Professor and President Hoshi University Tsuneji Nagai for their valuable assistance in my research work.

Also I wish to thank Dr. Kazuyo Yamada (Institute for Comprehensive Medical Science, Fujita Health University) and Dr. Kyoko Hayashi (Department of Virology, Toyama Medical and Pharmaceutical University) for their helpful assistance in my research work.

Moreover, I would like to thank Dr. Mariko Morishita, Dr. Yasuko Obata, and the member of the Department of Pharmaceutics for their kindness and friendship.

In addition, I would like to thank the members of Fine Drug Targeting Research Laboratory for their friendship and assistance.

I would like to thank Dr. Kazuyuki Shimizu, Dr. Sung Hee Hwang, and Dr. Koji Nakamura for their kindness and encouragement.

I wish to thank Mr. Hiroshi Soeda, Ms. Noriko Ogawa, Ms. Sae Yano, Ms. Rie Watai and Mr. Masato Watanabe for their assistance in the experimental work.

Finally, I will be forever in debt to my family for their support, words and comprehension.

REFERENCES

1) Nakanishi, T., Fukushima, S., Okamoto, K., Suzuki, M., Matsumura, Y., Yokoyama, M., Okano, T., Sakurai, Y., and Kataoka, K., Development of the polymer micelle carrier system for doxorubicin., *J. Control. Release*, 74, 295-302 (2001).

2) Constantinides, P. P., Lambert, K. J., Tustian, A. K., Schneider, B., Lalji, S., Ma, W., Wentzel, B., Kessler, D., Worah, D., and Quay, S. C., Formulation development and antitumor activity of a filter-sterilizable emulsion of paclitaxel., *Pharm. Res.*, 17, 175-182 (2000).

3) Yoo, H. S., Oh, J. E., Lee, K. H., and Park, T. G., Biodegradable nanoparticles containing doxorubicin-PLGA conjugate for sustained release., *Pharm. Res.*, **16**, 1114-1118 (1999).

4) Willis, M., and Forssen, E., Ligand-targeted liposomes., *Adv. Drug Deliv. Rev.*, **29**, 249-271 (1998).

5) Ishida, T., Kirchmeier, M. J., Moase, E. H., Zalipsky, S., and Allen, T. M., Targeted delivery and triggered release of liposomal doxorubicin enhances cytotoxicity against human B lymphoma cells., *Biochim. Biophys. Acta*, **1515**, 144-158 (2001).

6) Unezaki, S., Maruyama, K., Takahashi, N., Koyama, M., Yuda, T., Suginaka, A., and Iwatsuru, M., Enhanced delivery and antitumor activity of doxorubicin using long-circulating thermosensitive liposomes containing amphipathic polyethylene glycol in combination with local hyperthermia., *Pharm. Res.*, 11, 1180-1185 (1994).

7) Ishihara, H., Hayashi, Y., Hara, T., Aramaki, Y., Tsuchiya, S., and Koike, K., Specific uptake of asialofetuin-tacked liposomes encapsulating interferon-gamma by human hepatoma cells and its inhibitory effect on hepatitis B virus replication., *Biochem. Biophys. Res. Commun.*, 174, 839-845 (1991).

8) Wang, C. Y., and Huang, L., pH-sensitive immunoliposomes mediate target-cell-specific delivery and controlled expression of a foreign gene in mouse., *Proc. Natl. Acad. Sci. USA*, 84, 7851-7855 (1987).

9) Curiel, D. T., Agarwal, S., Wagner, E., and Cotten, M., Adenovirus enhancement of transferrin-polylysine-mediated gene delivery., *Proc. Natl. Acad. Sci. USA*, 88, 8850-8854 (1991).

10) Barratt, G., Tenu, J. P., Yapo, A., and Petit, J. F., Preparation and characterisation of liposomes containing mannosylated phospholipids capable of targetting drugs to macrophages., *Biochim. Biophys. Acta*, 862, 153-164 (1986).

11) Kawakami, S., Wong, J., Sato, A., Hattori, Y., Yamashita, F., and Hashida, M., Biodistribution characteristics of mannosylated, fucosylated, and galactosylated liposomes in mice., *Biochim. Biophys. Acta*, 1524, 258-265 (2000).

12) Goren, D., Horowitz, A. T., Tzemach, D., Tarshish, M., Zalipsky, S., and Gabizon, A., Nuclear delivery of doxorubicin via folate-targeted liposomes with bypass of multidrug-resistance efflux pump., *Clin. Cancer Res.*, 6, 1949-1957 (2000).

13) Versluis, A. J., Rensen, P. C., Rump, E. T., Van Berkel, T. J., and Bijsterbosch, M. K., Low-density lipoprotein receptor-mediated delivery

of a lipophilic daunorubicin derivative to B16 tumours in mice using apolipoprotein E-enriched liposomes., *Br. J. Cancer*, 78, 1607-1614 (1998).

14) Ashwell, G., and Harford, J., Carbohydrate-specific receptors of the liver., *Annu. Rev. Biochem.*, **51**, 531-554 (1982).

15) Schwartz, A. L., Rup, D., and Lodish, H. F., Difficulties in the quantification of asialoglycoprotein receptors on the rat hepatocyte., *J. Biol. Chem.*, **255**, 9033-9036 (1980).

16) Spanjer, H. H., and Scherphof, G. L., Targeting of lactosylceramide-containing liposomes to hepatocytes in vivo., *Biochim. Biophys. Acta*, **734**, 40-47 (1983).

17) Wu, J., Liu, P., Zhu, J. L., Maddukuri, S., and Zern, M. A., Increased liver uptake of liposomes and improved targeting efficacy by labeling with asialofetuin in rodents., *Hepatology*, **27**, 772-778 (1998).

18) Murahashi, N., Ishihara, H., Sasaki, A., Sakagami, M., and Hamana, H., Hepatic accumulation of glutamic acid branched neogalactosyllipid modified liposomes., *Biol. Pharm. Bull.*, **20**, 259-266 (1997).

19) Shimizu, K., Qi, X. R., Maitani, Y., Yoshii, M., Kawano, K., Takayama, K., and Nagai, T., Targeting of soybean-derived sterylglucoside liposomes to liver tumors in rat and mouse models., *Biol. Pharm. Bull.*, **21**, 741-746 (1998).

20) Shimizu, K., Maitani, Y., Takayama, K., and Nagai, T., Characterization of dipalmitoylphosphatidylcholine liposomes containing a soybean-derived sterylglucoside mixture by differential scanning calorimetry, Fourier transform infrared spectroscopy, and

enzymatic assay., *J. Pharm. Sci.*, 85, 741-744 (1996).

21) Kawaguchi, K., Kuhlenschmidt, M., Roseman, S., and Lee, Y. C., Differential uptake of D-galactosyl- and D-glucosyl-neoglycoproteins by isolated rat hepatocytes., *J. Biol. Chem.*, 256, 2230-2234 (1981).

22) Nishikawa, M., Ohtsubo, Y., Ohno, J., Fujita, T., Koyama, Y., Yamashita, F., Hashida, M., and Sezaki, H., Pharmacokinetics of receptor-mediated hepatic uptake of glycosylated albumin in mice., *Int. J. Pharm.*, 85, 75-85 (1992).

23) Maitani, Y., Nakamura, K., Suenaga, H., Kamata, K., Takayama, K., and Nagai, T., The enhancing effect of soybean-derived sterylglucoside and β-sitosterol β- D-glucoside on nasal absorption in rabbits., *Int. J. Pharm.*, 200, 17-26 (2000).

24) Imai, T., Sakai, M., Ohtake, H., Azuma, H., and Otagiri, M., In vitro and in vivo evaluation of the enhancing activity of glycyrrhizin on the intestinal absorption of drugs., *Pharm. Res.*, 16, 80-86 (1999).

25) Mishima, M., Okada, S., Wakita, Y., and Nakano, M., Promotion of nasal absorption of insulin by glycyrrhetinic acid derivatives. I., *J. Pharmacobiodyn.*, 12, 31-36 (1989).

26) Aungst, B. J., Rogers, N. J., and Shefter, E., Comparison of nasal, rectal, buccal, sublingual and intramuscular insulin efficacy and the effects of a bile salt absorption promoter., *J. Pharmacol. Exp. Ther.*, 244, 23-27 (1988).

27) Ogiso, T., Iwaki, M., Yoneda, I., Horinouchi, M., and Yamashita, K., Percutaneous absorption of elcatonin and hypocalcemic effect in rat., *Chem. Pharm. Bull.*, 39, 449-453 (1991).

28) Kramer, W., Wess, G., Schubert, G., Bickel, M., Girbig, F., Gutjahr, U., Kowalewski, S., Baringhaus, K. H., Enhsen, A., Glombik, H., Mullner, S., Neckermann, G., Schulz, S., and Petzinger, E., Liver-specific drug targeting by coupling to bile acids., *J. Biol. Chem.*, **267**, 18598-18604 (1992).

29) Osaka, S., Tsuji, H., and Kiwada, H., Uptake of liposomes surface-modified with glycyrrhizin by primary cultured rat hepatocytes., *Biol. Pharm. Bull.*, 17, 940-943 (1994).

30) Kimura, K., A phase II study of (2"R)-4'-*O*-tetrahydropyranyl-adriamycin (THP) in patients with hematological malignancies. THP Study Group., *Jpn. J. Cancer Chemother.*, 13, 368-375 (1986).

31) Saito, T., Kasai, Y., Wakui, A., Furue, H., Majima, H., Nitani, H., Niijima, T., Takeda, C., Abe, O., Koyama, Y., and et al., Phase II study of (2"R)-4'-*O*-tetrahydropyranyladriamycin (THP) in patients with solid tumors. Multi-Institutional Cooperative Study., *Jpn. J. Cancer Chemother.*, 13, 1060-1069 (1986).

32) Okuma, K., Furuta, I., and Ota, K., Acute cardiotoxicity of anthracyclines--analysis by using Holter ECG., *Jpn. J. Cancer Chemother.*, 11, 902-911 (1984).

33) Sugiyama, T., Sadzuka, Y., Nagasawa, K., Ohnishi, N., Yokoyama, T., and Sonobe, T., Membrane transport and antitumor activity of pirarubicin, and comparison with those of doxorubicin., *Jpn. J. Cancer Res.*, **90**, 775-780 (1999).

34) Kirby, C. J., and Gregoriadis, G., Dehydration-rehydration vesicles (DRV): A new method for high yield drug entrapment in liposomes.,

Biotechnology, **2**, 979-984 (1984).

35) Ciechanover, A., Schwartz, A. L., and Lodish, H. F., Sorting and recycling of cell surface receptors and endocytosed ligands: the asialoglycoprotein and transferrin receptors., *J. Cell Biochem.*, **23**, 107-130 (1983).

36) Ishihara, H., Hara, T., Aramaki, Y., Tsuchiya, S., and Hosoi, K., Preparation of asialofetuin-labeled liposomes with encapsulated human interferon-gamma and their uptake by isolated rat hepatocytes, *Pharm. Res.*, 7, 542-546 (1990).

37) Hara, T., Kuwasawa, H., Aramaki, Y., Takada, S., Koike, K., Ishidate, K., Kato, H., and Tsuchiya, S., Effects of fusogenic and DNA-binding amphiphilic compounds on the receptor-mediated gene transfer into hepatic cells by asialofetuin-labeled liposomes, *Biochim. Biophys. Acta*, **1278**, 51-58 (1996).

38) Kawakami, S., Yamashita, F., Nishikawa, M., Takakura, Y., and Hashida, M., Asialoglycoprotein receptor-mediated gene transfer using novel galactosylated cationic liposome, *Biochem. Biophys. Res. Commun.*, **252**, 78-83 (1998).

39) Shimizu, K., Maitani, Y., Takayama, K., and Nagai, T., Formulation of liposomes with a soybean-derived sterylglucoside mixture and cholesterol for liver targeting., *Biol. Pharm. Bull.*, **20**, 881-886 (1997).

40) Batzri, S., and Korn, E. D., Single bilayer liposomes prepared without sonication., *Biochim. Biophys. Acta*, **298**, 1015-1019 (1973).

41) Qi, X. R., Maitani, Y., Nagai, T., and Wei, S. L., Comparative pharmacokinetics and antitumor efficacy of doxorubicin encapsulated in

soybean-derived sterols and poly(ethylene glycol) liposomes in mice., *Int. J. Pharm.*, **146**, 31-39 (1997).

42) Stowell, C. P., and Lee, Y. C., The binding of D-glucosyl-neoglycoproteins to the hepatic asialoglycoprotein receptor., *J. Biol. Chem.*, **253**, 6107-6110 (1978).

43) Han, J., Lim, M., and Yeom, Y. I., Receptor-mediated gene transfer to cells of hepatic origin by galactosylated albumin-polylysine complexes., *Biol. Pharm. Bull.*, **22**, 836-840 (1999).

44) Schwartz, A. L., Fridovich, S. E., Knowles, B. B., and Lodish, H. F., Characterization of the asialoglycoprotein receptor in a continuous hepatoma line., *J. Biol. Chem.*, **256**, 8878-8881 (1981).

45) Han, J. H., Oh, Y. K., Kim, D. S., and Kim, C. K., Enhanced hepatocyte uptake and liver targeting of methotrexate using galactosylated albumin as a carrier., *Int. J. Pharm.*, **188**, 39-47 (1999).

46) Hara, T., Aramaki, Y., Takada, S., Koike, K., and Tsuchiya, S., Receptor-mediated transfer of pSV2CAT DNA to a human hepatoblastoma cell line HepG2 using asialofetuin-labeled cationic liposomes., *Gene*, **159**, 167-174 (1995).

47) Maitani, Y., Hwang, S. H., Tanaka, S., Takayama, K., and Nagai, T., Physicochemical characteristics and transfection efficiency of DNA in liposomes with soybean-derived sterylglucoside into HepG2 cells., *J. Pharm. Sci. Technol., Jpn.*, **61**, 1-10 (2001).

48) Hwang, S. H., Hayashi, K., Takayama, K., and Maitani, Y., Liver-targeted gene transfer into a human hepatoblastoma cell line and in vivo by sterylglucoside-containing cationic liposomes., *Gene Ther.*, **8**,

1276-1280 (2001).

49) Yachi, K., Suzuki, N., Tanaka, N., Okada, K., Mitsui, I., Kawato, Y., Komagata, Y., Komiyama, K., and Kikuchi, H., The effect of adriamycin against a liver metastatic model by encapsulation in liposomes., *Biopharm. Drug Dispos.*, 17, 699-715 (1996).

50) Muramatsu, K., Maitani, Y., Machida, Y., and Nagai, T., Effect of soybean-derived sterol and its glucoside mixtures on the stability of dipalmitoylphosphatidylcholine and dipalmitoylphosphatidylcholine/ cholesterol liposomes., *Int. J. Pharm.*, **107**, 1-8 (1994).

51) Szoka, F. C. Jr., Jacobson, K., and Papahadjopoulos, D., The use of aqueous space markers to determine the mechanism of interaction between phospholipid vesicles and cells., *Biochim. Biophys. Acta*, **551**, 295-303 (1979).

52) Horowitz, A. T., Barenholz, Y., and Gabizon, A. A., In vitro cytotoxicity of liposome-encapsulated doxorubicin: dependence on liposome composition and drug release., *Biochim. Biophys. Acta*, **1109**, 203-209 (1992).

53) Ando, T., Maitani, Y., Yamamoto, T., Takayama, K., and Nagai, T., Nasal insulin delivery in rabbits using soybean-derived sterylglucoside and sterol mixtures as novel enhancers in suspension dosage forms, *Biol. Pharm. Bull.*, **21**, 862-865 (1998).

54) Hall, D., Use of optical biosensors for the study of mechanistically concerted surface adsorption processes., *Anal Biochem*, **288**, 109-125 (2001).

55) Wang, L. Y., Ma, J. K., Pan, W. F., Toledo-Velasquez, D., Malanga, C. J.,

and Rojanasakul, Y., Alveolar permeability enhancement by oleic acid and related fatty acids: evidence for a calcium-dependent mechanism, *Pharm. Res.*, 11, 513-517 (1994).

56) Francoeur, M. L., Golden, G. M., and Potts, R. O., Oleic acid: Its effects on stratum corneum in relation to (trans) dermal drug delivery, *Pharm. Res.*, 7, 621-627 (1990).

57) Nakamura, K., Maitani, Y., and Takayama, K., The enhancing effect of nasal absorption of FITC-dextran 4,400 by β-sitosterol β-D-glucoside in rabbits., *J. Control. Release*, **79**, 147-155 (2002).

58) Iguchi, H., Tone, H., Ishikura, T., Takeuchi, T., and Umezawa, H., Pharmacokinetics and disposition of 4'-*O*-tetrahydropyranyladriamycin in mice by HPLC analysis., *Cancer Chemother. Pharmacol.*, **15**, 132-140 (1985).

59) Izumi, N., and Goto, Y., A clinical trial of transarterial chemoembolization for hepatocellular carcinoma using 4'-*O*-tetrahydropyranyladriamycin., *Jpn. J. Cancer Chemother.*, 17, 1303-1307 (1990).

60) Rougier, P., Munck, J. N., Elias, D., Herait, P., Bognel, C., Gosse, C., and Lasser, P., Intra-arterial hepatic chemotherapy with pirarubicin. Preclinical and clinical studies., *Am. J. Clin. Oncol.*, **13 Suppl 1**, S1-S4 (1990).

61) Ramirez, L. H., Munck, J. N., Bognel, C., Zhao, Z., Ardouin, P., Poupon, M. F., Gouyette, A., and Rougier, P., Pharmacology and antitumour effects of intraportal pirarubicin on experimental liver metastases., *Br. J. Cancer*, **68**, 277-281 (1993).

62) Maurer-Spurej, E., Wong, K. F., Maurer, N., Fenske, D. B., and Cullis, P. R., Factors influencing uptake and retention of amino-containing drugs in large unilamellar vesicles exhibiting transmembrane pH gradients., *Biochim. Biophys. Acta*, **1416**, 1-10 (1999).

63) Zadi, B., and Gregoriadis, G., A novel method for high-yield entrapment of solutes into small liposomes., *J. Liposome Res.*, **10**, 73-80 (2000).

64) Gregoriadis, G., Saffie, R., and Hart, S. L., High yield incorporation of plasmid DNA within liposomes: effect on DNA integrity and transfection efficiency., *J. Drug Target.*, 3, 469-475 (1996).

65) Matsushita, Y., Iguchi, H., Kiyosaki, T., Tone, H., Ishikura, T., Takeuchi, T., and Umezawa, H., A high performance liquid chromatographic method of analysis of 4'-*O*-tetrahydropyranyl-adriamycin and their metabolites in biological samples., *J. Antibiot.*, **36**, 880-886 (1983).

66) Morikawa, N., Mori, T., Takeyama, M., and Hori, S., Pharmacokinetics of intra-arterially administered pirarubicin in plasma and cerebrospinal fluid of patients with glioma., *Biol. Pharm. Bull.*, **21**, 297-299 (1998).

67) Yamaoka, K., Tanigawara, Y., Nakagawa, T., and Uno, T., A pharmacokinetic analysis program (multi) for microcomputer., *J. Pharmacobiodyn.*, 4, 879-885 (1981).

68) Crowe, J. H., and Crowe, L. M., Preservation of liposomes by freeze-drying., *in: G. Gregoriadis (Ed), Liposome Technology, Vol. I, 2nd Edition, CRC Press, Boca Raton, FL,*, 229-252 (1993).

69) Talmadge, J. E., Key, M. E., and Hart, I. R., Characterization of a murine ovarian reticulum cell sarcoma of histiocytic origin., *Cancer Res.*,

41, 1271-1280 (1981).

70) Hart, I. R., Talmadge, J. E., and Fidler, I. J., Metastatic behavior of a murine reticulum cell sarcoma exhibiting organ-specific growth., *Cancer Res.*, **41**, 1281-1287 (1981).

71) Fujita, H., Ogawa, K., Tone, H., Iguchi, H., Shomura, T., and Murata, S., Pharmacokinetics of doxorubicin, (2"R)-4'-*O*-tetrahydropyranyl-adriamycin and aclarubicin., *Jpn. J. Antibiot.*, **39**, 1321-1336 (1986).

72) Tone, H., Shirai, M., Onoue, F., and Kumagai, H., Toxicological studies on (2"R)-4'-*O*-tetrahydropyranyladriamycin, a new antitumor antibiotic. Acute toxicity study in mice., *Jpn. J. Antibiot.*, **39**, 250-258 (1986).